Inorg. Chem. **1984**, *23*, 1021-1037 **1021**

the Os_3 face which it occupies in its precursor, $CpWOs_3(CO)_{10}(\mu_3\text{-}\eta^2\text{-}C_2H_2)(\mu\text{-}H)$.

(2) The tungsten atom has a coordination shell consisting of $\eta^5\text{-}C_5H_5$, 3Os, σ-C, and $=$O. This pattern recurs in a number of other WOs_3 clusters that we are currently studying—viz., $CpWOs_3(CO)_9(\mu\text{-}O)(\mu_3\text{-}CCH_2C_6H_4Me)$,[29] which is formed by pyrolysis of $CpWOs_3(CO)_{11}(\mu_3\text{-}\eta^2\text{-}C(O)CH_2C_6H_4Me)$,[30,31] $CpWOs_3(CO)_9(\mu\text{-}O)(\mu\text{-}CHCH_2C_6H_4Me)(\mu\text{-}H)$,[32] and $CpWOs_3(CO)_9(\mu\text{-}O)(\mu_2\text{-}C{=}CHC_6H_4Me)(\mu\text{-}H)$.[33]

(3) The μ-O ligand must be a four-electron donor in order to satisfy the overall saturation of the compound. The W$=$O group acts as a two-electron donor to Os(1), which in turn acts as a donor to the tungsten atom in order to supply sufficient electrons to the latter:

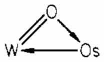

The source of the oxo ligand in **2** is not known. In order to determine whether Me_3NO is the source of the oxygen atom, the synthesis of **2** was carried out by using 2 equiv of Me_3NO. This reaction resulted in extensive decomposition and gave a much lower yield (12%) of **2**. The oxo ligand may be derived from a CO ligand by C–O bond scission or from other possible sources (O_2, H_2O, etc.). Note, however, that the oxo–alkylidyne species $CpWOs_3(CO)_9(\mu\text{-}O)(\mu_3\text{-}CCH_2C_6H_4Me)$ contains a similar oxo ligand acting as a four-electron donor across a tungsten–osmium linkage; in this case the oxo ligand and the alkylidyne ligand are produced from scission of a $\mu_3\text{-}\eta^2$-acyl ligand in the precursor, $CpWOs_3(CO)_{10}(\mu_3\text{-}\eta^2\text{-}C(O)CH_2C_6H_4Me)$.[29]

Acknowledgment. This research was supported at the State University of New York at Buffalo by National Science Foundation Grant CHE 80-23448 to M.R.C. and at the University of Illinois by National Science Foundation Grant CHE 81-00140 to J.R.S. Instruments at the University of Illinois supported by Grants NSF CHE 79-16100 and NIH GM 27029 were utilized for NMR and mass spectra, respectively.

Registry No. **1**, 89065-34-9; **2**, 89044-06-4; $CpWOs_3(CO)_{12}H$, 68796-10-1; W, 7440-33-7; Os, 7440-04-2.

Supplementary Material Available: A table of anisotropic thermal parameters (Table II-S) and a list of observed and calculated structure factor amplitudes (16 pages). Ordering information is given on any current masthead page.

---

[29] Shapley, J. R.; Park, J. T.; Churchill, M. R.; Ziller, J. W.; Beanan, L. R. *J. Am. Chem. Soc.*, in press (WOS7).

[30] Park, J. T.; Shapley, J. R.; Churchill, M. R.; Bueno, C. *Inorg. Chem.* **1983**, *22*, 1579.

[31] Shapley, J. R.; Park, J. T.; Churchill, M. R.; Bueno, C.; Wasserman, H. J. *J. Am. Chem. Soc.* **1981**, *103*, 7385.

[32] Churchill, M. R.; Li, Y. J.; Park, J. T.; Shapley, J. R., unpublished work (WOS8).

[33] Churchill, M. R.; Li, Y. J.; Park, J. T.; Shapley, J. R., unpublished work (WOS10-FRAN).

Contribution from the Department of Chemistry and Molecular Structure Center,
Indiana University, Bloomington, Indiana 47405

Reactions of Metal–Metal Multiple Bonds. 10.[1] Reactions of $Mo_2(OR)_6$ ($M\equiv M$) and $[Mo(OR)_4]_x$ Compounds with Molecular Oxygen. Preparation and Characterization of Oxo Alkoxides of Molybdenum: $MoO_2(OR)_2$, $MoO_2(OR)_2(bpy)$, $MoO(OR)_4$, $Mo_3O(OR)_{10}$, $Mo_4O_8(OR)_4(py)_4$, and $Mo_6O_{10}(OR)_{12}$

MALCOLM H. CHISHOLM,* KIRSTEN FOLTING, JOHN C. HUFFMAN, and CHARLES C. KIRKPATRICK

Received May 3, 1983

$Mo_2(OR)_6$ ($M\equiv M$) compounds and molecular oxygen react in hydrocarbon solvents to give $MoO_2(OR)_2$ compounds and alkoxy radicals. For R = *t*-Bu, the reaction is rapid with no isolable intermediates; for R = *i*-Pr and CH_2-*t*-Bu, intermediates of formulas $Mo_3O(OR)_{10}$ and $Mo_6O_{10}(O\text{-}i\text{-}Pr)_{12}$ have been isolated and characterized. $[Mo(OR)_4]_x$ compounds react with O_2 to give $MoO(OR)_4$ compounds where R = *t*-Bu and $x = 1$, R = *i*-Pr and $x = 2$, and R = CH_2-*t*-Bu and $x \geq 2$. $Mo(O\text{-}t\text{-}Bu)_4$ and O_2 also react to yield $MoO_2(O\text{-}t\text{-}Bu)_2$ and *t*-BuO· in a 1:2 ratio. A general scheme for the reaction of $Mo_2(OR)_6$ compounds with O_2 is proposed involving an initial facile cleavage of the $Mo\equiv Mo$ bond to give $MoO_2(OR)_2$ and $Mo(OR)_4$ compounds. The subsequent course of the reaction depends on the reactivity of $Mo(OR)_4$ compounds. The new oxo alkoxides $MoO_2(O\text{-}t\text{-}Bu)_2$, $MoO_2(OR)_2(bpy)$ (where R = *i*-Pr and CH_2-*t*-Bu), $Mo_3(\mu_3\text{-}O)(\mu_3\text{-}OR)(\mu\text{-}OR)_3(OR)_6$ (where R = *i*-Pr and CH_2-*t*-Bu), $Mo_4O_8(O\text{-}i\text{-}Pr)_4(py)_2$, and $Mo_6O_{10}(O\text{-}i\text{-}Pr)_{12}$ have been characterized by a variety of physicochemical techniques. The oxo groups are formed from the added molecular oxygen. Crystal data: (i) $MoO_2(O\text{-}i\text{-}Pr)_2(bpy)_2\cdot{}^1/_2$(toluene) at −161 °C, $a = 13.907$ (6) Å, $b = 8.413$ (3) Å, $c = 19.999$ (8) Å, $\alpha = 111.02$ (1)°, $\beta = 71.37$ (2)°, $\gamma = 88.98$ (1)°, $Z = 4$, $d_{calcd} = 1.455$ g cm^{-3}, space group $P\bar{1}$; (ii) $Mo_3O(OCH_2\text{-}t\text{-}Bu)_{10}\cdot{}^1/_3CH_2Cl_2$ at −161 °C, $a = 35.557$ (19) Å, $b = 18.969$ (9) Å, $c = 19.342$ (9) Å, $Z = 8$, $d_{calcd} = 1.283$ g cm^{-3}, space group *Pbcn*; (iii) $Mo_3O(O\text{-}i\text{-}Pr)_{10}$ at −162 °C, $a = 21.274$ (6) Å, $b = 21.808$ (5) Å, $c = 10.207$ (2) Å, $\alpha = 98.69$ (1)°, $\beta = 92.92$ (1)°, $\gamma = 118.03$ (1)°, $Z = 4$, $d_{calcd} = 1.452$ g cm^{-3}, space group $P\bar{1}$; (iv) $Mo_6O_{10}(O\text{-}i\text{-}Pr)_{12}$ at −162 °C, $a = 13.082$ (3) Å, $b = 11.478$ (2) Å, $c = 9.760$ (2) Å, $\alpha = 106.40$ (1)°, $\beta = 91.85$ (1)°, $\gamma = 99.81$ (1)°, $Z = 1$, $d_{calcd} = 1.738$ g cm^{-3}, space group $P\bar{1}$.

Introduction

We have shown that the $Mo\equiv Mo$ bond in $Mo_2(OR)_6$ compounds is labile toward a number of oxidative-addition reactions. Treatment with halogens leads to the formation of $Mo_2(OR)_6X_4$ (M–M) compounds (R = *i*-Pr; X = Cl, Br, I), and addition of ROOR to formation of $Mo_2(OR)_8$ (R = *i*-Pr).[2] Reaction with benzoyl peroxide gave[3] a compound $Mo_2(OR)_6(O_2CPh)_2$ (R = *i*-Pr), believed to contain a $Mo{=}Mo$ bond. These earlier findings prompted us to continue to in-

---

[1] Chisholm, M. H.; Huffman, J. C.; Ratermann, A. L. *Inorg. Chem.* **1983**, *22*, 4100.

[2] Chisholm, M. H.; Huffman, J. C.; Kirkpatrick, C. C. *Inorg. Chem.* **1981**, *20*, 871.

[3] Chisholm, M. H.; Huffman, J. C.; Kirkpatrick, C. C. *Inorg. Chem.* **1983**, *22*, 2903.

0020-1669/84/1323-1021$01.50/0

vestigate oxidative additions wtih simple X_2 molecules. We report here our studies involving molecular oxygen. Preliminary reports of certain aspects of this work have been published.[4-6]

Results and Discussion

Studies of the Reaction between $Mo_2(OR)_6$ and O_2. We have limited our studies to reactions where R = *t*-Bu, *i*-Pr, and CH_2-*t*-Bu. These three alkoxides are taken to be representative primary, secondary, and tertiary alkoxides for $Mo_2(OR)_6$ compounds, bearing in mind that steric bulk is required in order to suppress oligomerization to $[Mo(OR)_3]_x$.[7]

Mo_2(O-*t*-Bu)$_6$ + O_2. Orange hydrocarbon solutions of Mo_2(O-*t*-Bu)$_6$ fade slowly to pale yellow when stirred under 1 atm of dry molecular oxygen. From experiments employing a gas buret, the moles of O_2 consumed per mole of Mo_2(O-*t*-Bu)$_6$ is 2.0 ± 0.1. When the solvent is stripped, a thick yellow liquid remains that can be distilled at 50–55 °C (10^{-4} torr). Elemental analyses and all other characterization data indicate the yellow liquid is MoO_2(O-*t*-Bu)$_2$. When Mo_2(O-*t*-Bu)$_6$ is dissolved in benzene-d_6 or toluene-d_8 and sealed in an NMR tube under 1 atm of O_2, the ^{1}H NMR spectrum shows that MoO_2(O-*t*-Bu)$_2$ and *t*-BuOD are present in the molar ratio 1:1. The formation of *t*-BuOD was confirmed by two methods: (i) The NMR tube was opened, and an authentic sample of *t*-BuOH was added. (ii) The volatile components were vacuum distilled into another NMR tube. *t*-BuOD was the only organic product observed by ^{1}H NMR spectroscopy. In related NMR tube reactions, Mo_2(O-*t*-Bu)$_6$ and O_2 were allowed to react in toluene-d_8 in the presence of 1,4-cyclohexadiene. In these experiments, *t*-BuOH and benzene were the only organic products. Thus, the stoichiometry of the reaction shown in eq 1 is determined.

$$Mo_2(O\text{-}t\text{-}Bu)_6 + 2O_2 \rightarrow 2MoO_2(O\text{-}t\text{-}Bu)_2 + 2t\text{-}BuO\cdot \quad (1a)$$

$$2t\text{-}BuO\cdot +$$

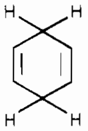

$$\rightarrow 2t\text{-}BuOH + C_6H_6 \quad (1b)$$

When Mo_2(O-*t*-Bu)$_6$ and O_2 were allowed to react in an ca. 1:1 mole ratio, only unreacted Mo_2(O-*t*-Bu)$_6$ and MoO_2(O-*t*-Bu)$_2$ and *t*-BuOH/D were detected by NMR spectroscopy. No intermediates have been detected in this reaction. Reactions involving $^{18}O_2$ yield $Mo^{18}O_2$(O-*t*-Bu)$_2$, thereby establishing the origin of the oxo ligands.

Mo_2(O-*i*-Pr)$_6$ + O_2. When hydrocarbon solutions of Mo_2(O-*i*-Pr)$_6$ are stirred under 1 atm of dry molecular oxygen, the color changes from yellow to green to brown and ultimately to pale yellow again. From experiments employing a gas buret, 2 equiv of O_2 are consumed/equiv of Mo_2(O-*i*-Pr)$_6$ over the entire reaction sequence. Although the ultimate product MoO_2(O-*i*-Pr)$_2$ is not easily isolated, being prone to apparent autocatalytic decomposition to molybdenum blue oxides, the addition of 2,2′-bipyridine, bpy, after the uptake of 2 equiv of O_2 allows the isolation of the Lewis base adduct MoO_2(O-*i*-Pr)$_2$(bpy). When Mo_2(O-*i*-Pr)$_6$ was dissolved in benzene-d_6 and allowed to react with O_2, the organic volatiles were identified as *i*-PrOH and Me_2CO by ^{1}H NMR spectroscopy and confirmed by the further addition of an authentic sample of each component. When a similar reaction was carried out in the presence of 1,4-cyclohexadiene, only *i*-PrOH and benzene were detected. Evidently, proton abstraction from 1,4-cyclohexadiene is favored over the bimolecular reaction of two *i*-PrO radicals, which gives *i*-PrOH and Me_2CO. The intermediates whose colors are observed prior to complete conversion to MoO_2(O-*i*-Pr)$_2$ are Mo_3O(O-*i*-Pr)$_{10}$ (green) and Mo_6O_{10}(O-*i*-Pr)$_{12}$ (dark yellow or brown). Both compounds were first isolated from reactions between Mo_2(O-*i*-Pr)$_6$ and less than 2 equiv of O_2 by crystallization.

Hydrocarbon solutions of Mo_2(O-*i*-Pr)$_6$, when treated with O_2 in the presence of added pyridine, initially turn red and then yellow as a relatively small quantity of red crystals are formed. The major products are MoO_2(O-*i*-Pr)$_2$(py)$_2$ and *i*-PrOH; MoO(O-*i*-Pr)$_4$(py) and the red crystalline precipitate Mo_4O_8(O-*i*-Pr)$_4$(py)$_4$ are the minor products in this reaction. No Mo_3O(O-*i*-Pr)$_{10}$ is formed when pyridine is present.

Mo_2(OCH_2-*t*-Bu)$_6$ + O_2. Hydrocarbon solutions of Mo_2(OCH_2-*t*-Bu)$_6$ change from yellow to green when treated with dry molecular oxygen. From experiments employing a gas buret, somewhat less than 2.0 equiv (ca. 1.8 equiv) of O_2 are consumed/equiv of Mo_2(OCH_2-*t*-Bu)$_6$. The major inorganic compound formed in this reaction is MoO_2(OCH_2-*t*-Bu)$_2$, which has been isolated as an adduct with bpy, MoO_2(OCH_2-*t*-Bu)$_2$(bpy), by the addition of bpy after the uptake of molecular oxygen had ceased. *t*-BuCH_2OH/D is the organic product that was identified by techniques analogous to those described before in the detection of *t*-BuOH and *i*-PrOH. A minor residual product, MoO(OCH_2-*t*-Bu)$_4$, has been detected by ^{1}H NMR spectroscopy and is probably responsible for the overall consumption of less than 2 equiv of O_2. The green compound, Mo_3O(OCH_2-*t*-Bu)$_{10}$, has been shown to be formed early in the reaction.

When molecular oxygen is allowed to react with Mo_2(OCH_2-*t*-Bu)$_6$ in the presence of pyridine, MoO_2(OCH_2-*t*-Bu)$_2$(py)$_2$ and *t*-BuCH_2OH are the only products formed. No Mo_3O(OCH_2-*t*-Bu)$_{10}$ was detected.

The aforementioned findings led us to suspect that Mo(IV) alkoxides, $[Mo(OR)_4]_x$, might be involved as reactive intermediates in the reactions involving $Mo_2(OR)_6$ compounds and O_2.

Reactions of $[Mo(OR)_4]_x$ Compounds with O_2. Mo(O-*t*-Bu)$_4$ + O_2. When hydrocarbon solutions of Mo(O-*t*-Bu)$_4$[8] are exposed to 1 atm of O_2, the products depend upon the initial concentration of the Mo(IV) alkoxide. MoO(O-*t*-Bu)$_4$ is the major product from concentrated solutions of Mo(O-*t*-Bu)$_4$ (>0.25 M), while MoO_2(O-*t*-Bu)$_2$ and *t*-BuOH are the products from dilute solutions (<0.001 M). A very plausible interpretation of this concentration effect may be based on the reactions shown in eq 2.

$$Mo(O\text{-}t\text{-}Bu)_4 + O_2 \rightarrow [Mo(O\text{-}t\text{-}Bu)_4O_2]^{\ddagger} \quad (2a)$$

$$[Mo(O\text{-}t\text{-}Bu)_4O_2]^{\ddagger} + Mo(O\text{-}t\text{-}Bu)_4 \rightarrow 2MoO(O\text{-}t\text{-}Bu)_4 \quad (2b)$$

$$[Mo(O\text{-}t\text{-}Bu)_4O_2]^{\ddagger} \rightarrow MoO_2(O\text{-}t\text{-}Bu)_2 + 2t\text{-}BuO\cdot \quad (2c)$$

At high initial Mo(O-*t*-Bu)$_4$ concentrations, the bimolecular pathway, eq 2b, leading to MoO(O-*t*-Bu)$_4$ is favored. Dilute solutions of Mo(O-*t*-Bu)$_4$ suppress the bimolecular pathway, eq 2b, and the products result from decomposition of the proposed dioxygen adduct, [Mo(O-*t*-Bu)$_4O_2$].

The steps proposed in eq 2 are similar to those proposed for oxygenation of a number of inorganic compounds. For example, Lever[9] has shown that PcMn(O_2), where Pc = phthalocyanine, forms when solutions of PcMn^{II} are exposed

---

(4) Chisholm, M. H.; Folting, K.; Huffman, J. C.; Kirkpatrick, C. C.; Ratermann, A. R. *J. Am. Chem. Soc.* **1981**, *103*, 1305.

(5) Chisholm, M. H.; Folting, K.; Huffman, J. C.; Kirkpatrick, C. C. *J. Am. Chem. Soc.* **1981**, *103*, 5397.

(6) Chisholm, M. H.; Folting, K.; Huffman, J. C.; Kirkpatrick, C. C. *J. Chem. Soc., Chem. Commun.* **1982**, 189.

(7) Chisholm, M. H.; Cotton, F. A.; Murillo, C. A.; Reichert, W. W. *Inorg. Chem.* **1977**, *16*, 1801.

(8) Chisholm, M. H.; Reichert, W. W.; Thornton, P. *J. Am. Chem. Soc.* **1978**, *100*, 2744.

(9) Lever, A. P. B.; Wilshire, J. P.; Whan, S. K. *Inorg. Chem.* **1981**, *20*, 761.

to O_2. Excess $PcMn^{II}$ reacts with the oxygen adduct to form $PcMnO_2MnPc$, which cleaves to give 2 equiv of PcMnO. Likewise, Balch[10] has shown that (P)Fe, where P = a porphyrin dianion, forms a dimer when exposed to O_2. The dimer then cleaves to form the mononuclear complex (P)FeO. Finally, Ledon[11] has reported the formation of a *cis*-dioxo complex, $MoO_2(TPP)$, where TPP = the tetraphenylporphyrin dianion, from a peroxo compound, $Mo(O_2)(TPP)$. The latter compound was generated by photolysis of a diperoxymolybdenum porphyrin, $Mo(O_2)_2(TPP)$.

$Mo_2(O\text{-}i\text{-}Pr)_8$ (M=M) + O_2. Hydrocarbon solutions of $Mo_2(O\text{-}i\text{-}Pr)_8$ react very rapidly with molecular oxygen to cleave the M–M double bond[12] and form 2 equiv of $MoO(O\text{-}i\text{-}Pr)_4$ according to eq 3.

$$Mo_2(O\text{-}i\text{-}Pr)_8 + O_2 \rightarrow 2MoO(O\text{-}i\text{-}Pr)_4 \quad (3)$$

The stoichiometry of the uptake of O_2 was determined by experiments employing a gas buret. Reaction 3 is a metathesis reaction: M=M and O=O bonds react to give two M=O bonds.

When $Mo_2(O\text{-}i\text{-}Pr)_8$ is dissolved in pyridine, the blue color, which is believed to be associated with the Mo=Mo bond, disappears, yielding a brown solution that is paramagnetic. $Mo(O\text{-}i\text{-}Pr)_4(py)_2$ is believed to be formed and is probably closely related to the well-characterized compounds $Mo(OSiR_3)_4(HNMe_2)_2$, where R = Me and Et.[8] The reaction between $Mo_2(O\text{-}i\text{-}Pr)_8$ dissolved in pyridine, $[Mo(O\text{-}i\text{-}Pr)_4(py)_2]$, and molecular oxygen proceeds according to eq 4. The isopropoxy radicals decompose to *i*-PrOH and Me_2CO as noted before.

$$Mo_2(O\text{-}i\text{-}Pr)_8 + py\ (excess) + O_2 \rightarrow 2MoO_2(O\text{-}i\text{-}Pr)_2(py)_2 + 4i\text{-}PrO\cdot \quad (4)$$

$[Mo(OCH_2\text{-}t\text{-}Bu)_4]_x$ + O_2. Whether $Mo(OCH_2\text{-}t\text{-}Bu)_4$ is a dimer or higher polymer in solution is not clear from magnetic and cryoscopic molecular weight data.[8] However, hydrocarbon solutions of $[Mo(OCH_2\text{-}t\text{-}Bu)_4]_x$ react rapidly with O_2 to yield $MoO(OCH_2\text{-}t\text{-}Bu)_4$ according to the stoichiometric reaction (5). Uptake of O_2 was determined by gas buret experiments.

$$[Mo(OCH_2\text{-}t\text{-}Bu)_4]_x + (x/2)O_2 \rightarrow xMoO(OCH_2\text{-}t\text{-}Bu)_4 \quad (5)$$

Alternate Syntheses of New Oxo Alkoxides. $MoO_2(OR)_2$ (R = *i*-Pr, CH_2-*t*-Bu). Undoubtedly the quickest and cleanest syntheses of $MoO_2(OR)_2$ compounds (R = *i*-Pr, CH_2-*t*-Bu) is by the alcoholysis reaction shown in eq 6.

$$MoO_2(O\text{-}t\text{-}Bu)_2 + ROH\ (excess) \rightarrow MoO_2(OR)_2 + 2t\text{-}BuOH \quad (6)$$

This avoids the slow reactions of the intermediates $Mo_3O(OR)_{10}$ and $Mo_6O_{10}(O\text{-}i\text{-}Pr)_{12}$ with O_2 when the $Mo_2(OR)_6$ compounds are used.

$Mo_3O(OR)_{10}$ (R = *i*-Pr, CH_2-*t*-Bu). These compounds contain a triangulo $Mo_3(12+)$ unit capped by an oxo and an alkoxy ligand. A straightforward and quantitative synthesis of these compounds is given by eq 7.

$$Mo_2(OR)_6 + MoO(OR)_4 \rightarrow Mo_3O(OR)_{10} \qquad R = i\text{-}Pr,\ CH_2\text{-}t\text{-}Bu \quad (7)$$

This synthesis has an analogy with the assembly of small clusters employing $M{=}CR_2$ and $M{\equiv}CR$ groups that has been exploited very successfully by Stone and co-workers.[13] In eq 7, the six electrons of the Mo≡Mo bond are redistributed to form three Mo–Mo single bonds ($a^2 + e^4$).

Reaction 7 is greatly influenced by the steric bulk of the R groups and by the choice of solvent. In pyridine or even hydrocarbon solutions containing pyridine, $Mo_2(OR)_6$ and $MoO(OR)_4$ do not react, presumably because pyridine coordinates to each and blocks the associative reaction. However, the compounds $Mo_3O(OR)_{10}$ once formed are quite stable toward pyridine and other donor ligands. They do not dissociate to $Mo_2(OR)_6$ and $MoO(OR)_4$ compounds. The importance of steric factors is seen in the fact that $Mo_2(O\text{-}t\text{-}Bu)_6$ and $MoO(O\text{-}t\text{-}Bu)_4$ do not react; similarly, $Mo_2(O\text{-}i\text{-}Pr)_6$ does not react with $MoO(O\text{-}t\text{-}Bu)_4$, nor does $Mo_2(O\text{-}t\text{-}Bu)_6$ react with $MoO(O\text{-}i\text{-}Pr)_4$.

$Mo_6O_{10}(O\text{-}i\text{-}Pr)_{12}$. This compound was first discovered as an intermediate in the reaction between $Mo_2(O\text{-}i\text{-}Pr)_6$ and O_2. It was isolated as a crystalline precipitate from hydrocarbon solutions because it is appreciably less soluble than the other oxo alkoxides present in solution. However, we have found cleaner and more direct syntheses, shown in eq 8 and 9.

$$Mo_3O(O\text{-}i\text{-}Pr)_{10} + 8MoO_2(O\text{-}i\text{-}Pr)_2 \rightarrow {}^3/_2Mo_6O_{10}(O\text{-}i\text{-}Pr)_{12} + 2MoO(O\text{-}i\text{-}Pr)_4 \quad (8)$$

$$Mo_2(O\text{-}i\text{-}Pr)_8 + 6MoO_2(O\text{-}i\text{-}Pr)_2 \rightarrow Mo_6O_{10}(O\text{-}i\text{-}Pr)_{12} + 2MoO(O\text{-}i\text{-}Pr)_4 \quad (9)$$

Both reactions appear quantitative by ^1H NMR studies, and $MoO(O\text{-}i\text{-}Pr)_4$ and $Mo_6O_{10}(O\text{-}i\text{-}Pr)_{12}$ are easily separated because the former is extremely soluble in hexane and the latter almost insoluble.

In both eq 8 and 9, molybdenum(IV) is being used to reduce $MoO_2(O\text{-}i\text{-}Pr)_2$ and facile oxo and alkoxide ligand-transfer reactions must occur. In eq 9, a plausible first step would involve the formation of a coordinatively unsaturated species $MoO(O\text{-}i\text{-}Pr)_2$ that could then associate with $MoO_2(O\text{-}i\text{-}Pr)_2$ (eq 10).

$$^1/_2Mo_2(O\text{-}i\text{-}Pr)_8 + MoO_2(O\text{-}i\text{-}Pr)_2 \rightarrow MoO(O\text{-}i\text{-}Pr)_2 + MoO(O\text{-}i\text{-}Pr)_4 \quad (10a)$$

$$MoO(O\text{-}i\text{-}Pr)_2 + 2MoO_2(O\text{-}i\text{-}Pr)_2 \rightarrow {}^1/_2Mo_6O_{10}(O\text{-}i\text{-}Pr)_{12} \quad (10b)$$

In reaction 8, the triangulo $Mo_3(12+)$ complex acts as a reducing agent, and a similar sequence shown in eq 11 can be envisaged to give rise to $Mo_6O_{10}(O\text{-}i\text{-}Pr)_{12}$.

$$Mo_3O(O\text{-}i\text{-}Pr)_{10} + MoO_2(O\text{-}i\text{-}Pr)_2 \rightarrow Mo_2O_3(O\text{-}i\text{-}Pr)_4 + Mo_2(O\text{-}i\text{-}Pr)_8 \quad (11a)$$

$$Mo_2O_3(O\text{-}i\text{-}Pr)_4 + MoO_2(O\text{-}i\text{-}Pr)_2 \rightarrow {}^1/_2Mo_6O_{10}(O\text{-}i\text{-}Pr)_{12} \quad (11b)$$

$Mo_2(O\text{-}i\text{-}Pr)_8$, formed in eq 11a, would react with $MoO_2(O\text{-}i\text{-}Pr)_2$ to give $Mo_6O_{10}(O\text{-}i\text{-}Pr)_{12}$ by the sequence shown in eq 10.

Related oxygen atom transfer reactions have been previously documented. For example, $MoO_2(acac)_2$ and $MoCl_2(acac)_2$ react[14] to give MoOCl(acac), and $W(CO)(C_2H_2)(S_2CNR_2)_2$ and $Mo_2O_3(S_2P(OEt)_2)_4$ react[15] to yield $WO(C_2H_2)(S_2CNR_2)_2$ and $MoO(S_2P(OEt)_2)_2$ (2 equiv) with the liberation of CO.

---

(10) Chin, D. H.; LaMar, G. N.; Balch, A. L. *J. Am. Chem. Soc.* **1980**, *102*, 5947.

(11) Ledon, H. J.; Bonnet, M.; Galland, D. *J. Am. Chem. Soc.* **1981**, *103*, 6209.

(12) Chisholm, M. H.; Cotton, F. A.; Extine, M. W.; Reichert, W. W. *Inorg. Chem.* **1978**, *17*, 2944.

(13) Ashworth, T. V.; Chetcuti, M. J.; Farrugia, L. J.; Howard, J. A. K.; Jeffrey, J. C.; Mills, R.; Pain, G. N.; Stone, F. G. A.; Woodward, P. *ACS Symp. Ser.* **1981**, *No. 155*, Chapter 15.

(14) Chen, G. J.-J.; McDonald, J. W.; Newton, W. E. *Inorg. Chim. Acta* **1979**, *35*, 93.

(15) Templeton, J. L.; Bennett, C. W.; Chen, G. J.-J.; McDonald, J. W.; Newton, W. E. *Inorg. Chem.* **1981**, *20*, 1248.

$Mo_4O_8(O\text{-}i\text{-}Pr)_4(py)_4$. The $Mo_4O_8(O\text{-}i\text{-}Pr)_4(py)_4$ cluster is synthesized in high yield by the addition of pyridine to a toluene solution of $Mo_6O_{10}(O\text{-}i\text{-}Pr)_{12}$, eq 12.

$$Mo_6O_{10}(O\text{-}i\text{-}Pr)_{12} + \text{py (excess)} \rightarrow Mo_4O_8(O\text{-}i\text{-}Pr)_4(py)_4 + 2MoO(O\text{-}i\text{-}Pr)_4(py) \quad (12)$$

When this reaction is carried out in an NMR tube with toluene-d_8 as solvent, the $Mo_4O_8(O\text{-}i\text{-}Pr)_4(py)_4$ cluster precipitates from solution and $MoO(O\text{-}i\text{-}Pr)_4(py)$ is the only species detectable by NMR spectroscopy.

As is discussed subsequently, $Mo_6O_{10}(O\text{-}i\text{-}Pr)_{12}$ is extensively dissociated in solution (benzene, toluene). Since the solutions remain diamagnetic, we propose that chain cleavage occurs with retention of the Mo–Mo single bonds. From a consideration of the structure of $Mo_6O_{10}(O\text{-}i\text{-}Pr)_{12}$, it is easy to envisage a reaction with pyridine in which the two terminal molybdenum atoms form $MoO(O\text{-}i\text{-}Pr)_4(py)$ and the central portion of the molecule forms 2 equiv of I.

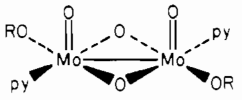

I

Two molecules of I may then associate to give II with the

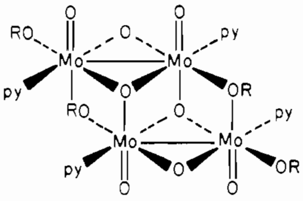

II

formation of two μ_3-oxo groups and two μ-OR groups. The square-based pyramidal coordination for molybdenum in I is transformed to octahedral coordination in II, but with retention of the Mo–Mo single bonds.

$Mo_2(OR)_6 + O_2$: A General Reaction Scheme. It is possible to envisage an overall scheme of reactions involving $Mo_2(OR)_6$ compounds and molecular oxygen leading to $MoO_2(OR)_2$ compounds based on an initial facile cleavage of the Mo≡Mo bond, eq 13.

$$Mo_2(OR)_6 + O_2 \rightleftharpoons [Mo_2(OR)_6(O_2)]^{\ddagger} \rightarrow MoO_2(OR)_2 + Mo(OR)_4 \quad (13)$$

It may be noted that a number of other small molecules (CO, HC≡CH) react with $Mo_2(OR)_6$ compounds to form reactive 1:1 adducts.[16,17] Disproportionation reactions have been observed, and from the reaction between $Mo_2(O\text{-}t\text{-}Bu)_6$ and CO, $Mo(O\text{-}t\text{-}Bu)_4$ has been isolated.[18]

The $Mo(OR)_4$ molecule formed in eq 13 may react in a number of ways: (1) It may react with O_2 as outlined in eq 2a–c. (2) It may associate to form $Mo_2(O\text{-}i\text{-}Pr)_8$ or $[Mo(OCH_2\text{-}t\text{-}Bu)_4]_x$, which then may react with O_2 to give $MoO(OR)_4$ compounds. Alternatively, $[Mo(OR)_4]_x$ may react with $MoO_2(OR)_2$ to give $Mo_6O_{10}(O\text{-}i\text{-}Pr)_{12}$ and $MoO(O\text{-}i\text{-}Pr)_4$, eq 9. (3) The $MoO(OR)_4$ compounds may react with $M_2(OR)_6$ to yield $Mo_3O(OR)_{10}$ compounds, when R = *i*-Pr and CH_2-*t*-Bu. However, in the absence of reduced molybdenum alkoxides, $MoO(OR)_4$ compounds become ultimate products along with $MoO_2(OR)_2$ compounds. (4) $Mo_3O(OR)_{10}$ compounds (R = *i*-Pr, CH_2-*t*-Bu) react directly with O_2, leading to RO· and $MoO_2(OR)_2$. (This reaction remains to be studied in detail.) $Mo_3O(OR)_{10}$ compounds also react with $MoO_2(OR)_2$ compounds to give $Mo_6O_{10}(O\text{-}i\text{-}Pr)_{12}$, which, being dissociatively labile, may be viewed as a source of two $MoO(O\text{-}i\text{-}Pr)_4$ molecules and two $Mo_2O_4(O\text{-}i\text{-}Pr)_2$ fragments. (5) $Mo_6O_{10}(O\text{-}i\text{-}Pr)_{12}$, which contains two Mo–Mo single bonds, behaves as a four-electron reductant in a final reaction with O_2, yielding $MoO_2(O\text{-}i\text{-}Pr)_2$.

Table I. Physical Characteristics of Oxy–Alkoxy–Molybdenum Compounds

compd	phys state (25 °C)	color	volatility,[a] °C	mol wt[b]
$MoO_2(O\text{-}t\text{-}Bu)_2$	liquid	yellow	55	267 ± 13 (274)
$MoO_2(O\text{-}t\text{-}Bu)_2(bpy)$	solid	white	d	
$MoO_2(O\text{-}i\text{-}Pr)_2(bpy)$	solid	white	d	
$MoO_2(OCH_2\text{-}t\text{-}Bu)_2(bpy)$	solid	white	d	
$MoO(O\text{-}t\text{-}Bu)_4$	liquid	yellow	85	
$MoO(O\text{-}i\text{-}Pr)_4$	liquid	yellow	60	410 ± 30 (348)
$MoO(OCH_2\text{-}t\text{-}Bu)_4$	solid	yellow	70	499 ± 50 (460)
$Mo_3O(O\text{-}i\text{-}Pr)_{10}$	solid	green	d	
$Mo_3O(OCH_2\text{-}t\text{-}Bu)_{10}$	solid	green	d	
$Mo_6O_{10}(O\text{-}i\text{-}Pr)_{12}$	solid	yellow	d	483 ± 50 (1444)
$Mo_4O_8(O\text{-}i\text{-}Pr)_4(py)_4\cdot 2py$	solid	red	d	

[a] Boiling point at 10^{-4} torr for liquids; sublimation temperature for solids at 10^{-4} torr; d = decomposes. [b] Cryoscopic determination in benzene: found (calcd based on formula).

Table II. Analytical Data for Oxy–Alkoxy–Molybdenum Compounds

compd	found %C	found %H	found %N	calcd %C	calcd %H	calcd %N
$MoO_2(O\text{-}t\text{-}Bu)_2$	35.45	6.98		35.05	6.62	
$MoO_2(O\text{-}t\text{-}Bu)_2(bpy)$	50.03	5.93	6.67	50.24	6.09	6.51
$MoO_2(O\text{-}i\ Pr)_2(bpy)$	47.79	5.34	7.09	47.76	5.51	6.96
$MoO_2(OCH_2\text{-}t\text{-}Bu)_2(bpy)$	52.14	6.73	6.03	52.40	6.60	6.11
$MoO(O\text{-}t\text{-}Bu)_4$	47.33	8.81		47.52	8.97	
$MoO(O\text{-}i\text{-}Pr)_4$	41.11	7.90		41.38	8.10	
$MoO(OCH_2\text{-}t\text{-}Bu)_4$	51.84	9.42		52.16	9.63	
$Mo_3O(O\text{-}i\ Pr)_{10}$	40.17	7.71		40.27	7.89	
$Mo_3O(OCH_2\text{-}t\text{-}Bu)_{10}$	50.83	9.17		51.10	9.43	
$Mo_6O_{10}(O\text{-}i\text{-}Pr)_{12}$	29.52	5.66		29.93	5.86	
$Mo_4O_8(O\text{-}i\text{-}Pr)_4(py)_4\cdot 2py$	41.17	4.83	6.71	41.15	5.00	6.61

A number of qualitative statements concerning relative rates and product distributions can be made on the basis of steric factors of the RO ligands that greatly influence the fate of the Mo(IV) alkoxy intermediates. However, these are speculative and are not presented here.

Characterization of Oxo–Alkoxy–Molybdenum Compounds. Some fundamental characterization properties of the oxo–alkoxy–molybdenum compounds are reported in Table I. Analytical data are given in Table II. ^1H NMR data and ^{17}O chemical shifts for representative terminal oxo groups are given in Table III. Stretching frequencies for terminal Mo=O groups are given in Table IV. Other characterization data are recorded in the Experimental Section or discussed in the following sections.

Solution and Physicochemical Properties of Mo(6+) Compounds. $MoO_2(O\text{-}t\text{-}Bu)_2$ is a yellow liquid, distillable at 55 °C (10^{-4} torr). It is stable under a dry atmosphere of oxygen or nitrogen but quickly decomposes to blue molybdenum oxides when exposed to moisture. The ^{17}O and ^1H NMR spectra indicate only one type of oxo and alkoxy group are present in the molecule. The ^{17}O chemical shift of the oxo ligand, 862 ppm downfield from $H_2{}^{17}O$, is well within the range of terminal oxo ligands for Mo(6+)-containing compounds.[19] The peak width at half height for the ^{17}O signal at 862 ppm is 90 Hz,

---

(16) Chisholm, M. H.; Huffman, J. C.; Leonelli, J.; Rothwell, I. P. *J. Am. Chem. Soc.* **1982**, *104*, 7030.

(17) Chisholm, M. H.; Folting, K.; Huffman, J. C.; Rothwell, I. P. *J. Am. Chem. Soc.* **1982**, *104*, 4389.

(18) Chisholm, M. H.; Cotton, F. A.; Extine, M. W.; Kelly, R. L. *J. Am. Chem. Soc.* **1979**, *101*, 7645.

(19) Klemperer, W. G. *Angew. Chem., Int. Ed. Engl.* **1978**, *17*, 246.

Table III. ^{17}O and ^{1}H NMR Data for Oxy–Alkoxy–Molybdenum Compounds

compd	$\delta(^{17}O)$ ($\Delta\gamma$)[a]	$\delta(^{1}H)$[b]
$MoO_2(O\text{-}t\text{-}Bu)_2$	862 (90)	1.20
$MoO_2(O\text{-}t\text{-}Bu)_2(py)_2$	885 (119)	8.50 (m, 2 H), 6.99 (m, 1 H), 6.68 (m, 2 H), 1.02 (s, 9 H)
$MoO_2(O\text{-}t\text{-}Bu)_2(bpy)$		8.55 (m, 1 H), 7.22 (m, 1 H), 7.12 (m, 1 H), 6.69 (m, 1 H), 1.18 (s, 9 H)
$MoO_2(O\text{-}i\text{-}Pr)_2(py)_2$	878 (32)	8.53 (m, 2 H), 6.99 (m, 1 H), 6.68 (m, 2 H), 4.77 (sept, 1 H), 1.30 (d, 6 H)
$MoO_2(O\text{-}i\text{-}Pr)_2(bpy)$		8.52 (m, 1 H), 7.20 (m, 1 H), 7.10 (m, 1 H), 6.66 (m, 1 H), 4.63 (sept, 1 H), 1.02 (d, 6 H)
$MoO_2(OCH_2\text{-}t\text{-}Bu)_2(py)_2$	872 (330)	8.53 (m, 2 H), 6.99 (m, 1 H), 6.65 (m, 2 H), 3.80 (s, 2 H), 0.60 (s, 9 H)
$MoO_2(OCH_2\text{-}t\text{-}Bu)_2(bpy)$		8.49 (m, 1 H), 7.18 (m, 1 H), 7.12 (m, 1 H), 6.99 (m, 1 H), 3.86 (s, 2 H), 0.68 (s, 9 H)
$MoO(O\text{-}t\text{-}Bu)_4$	970 (224)	1.45
$MoO(O\text{-}i\text{-}Pr)_4$	894 (150)	4.77 (sept, 1 H), 1.34 (d, 6 H)
$MoO(OCH_2\text{-}t\text{-}Bu)_4$		4.54 (s, 2 H), 1.04 (s, 9 H)
$Mo_3O(O\text{-}i\text{-}Pr)_{10}$		5.67 (sept, 2 H), 5.42 (sept, 3 H), 4.64 (sept, 3 H), 4.00 (sept, 1 H), 1.64 (d, 18 H), 1.57 (s, 18 H), 1.19 (sept, 6 H), 1.16 (s, 18 H)
$Mo_3O(OCH_2\text{-}t\text{-}Bu)_{10}$		4.87 (s, 6 H), 4.76 (s, 6 H), 4.14 (s, 6 H), 3.84 (s, 2 H), 1.02 (s, 27 H), 1.13 (s, 27 H), 0.999 (s, 27 H), 0.931 (s, 9 H)
$Mo_6O_{10}(O\text{-}i\text{-}Pr)_{12}$		5.18, 3.54, 1.50, 1.16 (all broad), 4.30 (sept, 1 H),[c] 1.30 (d, 6 H)[c]

[a] Chemical shifts are downfield from $H_2{}^{17}O$. All peak widths at half height are given in Hz. Spectra are recorded at 35 °C in toluene. No signals were observed for alkoxide oxygens. [b] Chemical shifts are downfield from Me_4Si. Parenthetic values give peak multiplicity, followed by relative proton integration. All spectra are recorded in toluene-d_8 at 16 °C, unless otherwise stated. s = singlet, d = doublet, sept = septet, m = multiplet. [c] At 75 °C.

Table IV. Terminal Molybdenum–Oxygen Stretching Frequencies for Oxo–Alkoxy–Molybdenum Compounds

compd	$\bar{\nu}(Mo\text{–}{}^{16}O)$, cm^{-1}	$\bar{\nu}(Mo\text{–}{}^{18}O)$, cm^{-1}
$MoO_2(O\text{-}t\text{-}Bu)_2$[a]	968, 930	920, 887
$MoO_2(O\text{-}t\text{-}Bu)_2(bpy)$[b]	912, 888	863, 843
$MoO_2(O\text{-}i\text{-}Pr)_2(bpy)$[b]	899, 880	
$MoO_2(OCH_2\text{-}t\text{-}Bu)_2(bpy)$[b]	918, 893	872, 851
$MoO(O\text{-}t\text{-}Bu)_4$[a]	967	
$MoO(O\text{-}i\text{-}Pr)_4$[a]	951	
$MoO(OCH_2\text{-}t\text{-}Bu)_4$[b]	915	
$Mo_4O_8(O\text{-}i\text{-}Pr)_4(py)_4$[b]	951, 918	904, 873

[a] Taken as a neat liquid between CsI plates. [b] Taken as a Nujol mull between CsI plates.

indicative of a monomeric species in solution.[19] This is also confirmed by a cryoscopic molecular weight determination in benzene. In the infrared spectrum, $MoO_2(O\text{-}t\text{-}Bu)_2$ shows two bands at 968 and 930 cm^{-1}, assignable to antisymmetric and symmetric Mo═O stretches, respectively. Upon ^{18}O-labeling ($Mo_2(O\text{-}t\text{-}Bu)_6 + {}^{18}O_2 \rightarrow Mo^{18}O_2(O\text{-}t\text{-}Bu)_2$), these bands shift to 920 and 887 cm^{-1}, respectively. $MoO_2(O\text{-}t\text{-}Bu)_2$ is therefore formulated as a molecule with virtual C_{2v} symmetry; it may be thought of as a dialkylated derivative of $MoO_4{}^{2-}$, namely the *tert*-butyl ester of molybdic acid.

$MoO_2(OR)_2$, where R = *i*-Pr and CH_2-*t*-Bu, are white solids that are only sparingly soluble in pentane and hexane. When crystallized from either solvent, filtered, and dried in vacuo, they decompose to blue molybdenum oxides. They can be kept in hydrocarbon solutions for a much longer time without decomposition, however.

$MoO_2(OR)_2(py)_2$ and $MoO_2(OR)_2(bpy)$ (R = *i*-Pr, CH_2-*t*-Bu). The pyridine adducts of $MoO_2(OR)_2$ are yellow liquids that lose pyridine upon heating under vacuum. Their spectroscopic properties indicate that they have essentially the same MoO_4N_2 geometry found for the related bpy adducts.

$MoO_2(OR)_2(bpy)$ compounds (R = *i*-Pr, CH_2-*t*-Bu) are white, air-sensitive solids that are soluble in chlorocarbon solvents but only sparingly soluble in hydrocarbon solvents.

^{17}O NMR spectra for $MoO_2(OR)_2(py)_2$ and $MoO_2(OR)_2(bpy)$ show only one signal in the range of terminal oxo groups, and the line width is sufficiently narrow to indicate monomeric species.

Kidd[20] has shown that, for a series of oxo–chromium(6+) compounds, a linear correlation exists between M–O π-bond order and ^{17}O chemical shift: increasing π-bond order increases the paramagnetic screening of the oxygen nucleus and results in a larger chemical shift (relative to $H_2{}^{17}O$). Reilley[21] demonstrated that a nonlinear correlation exists between ^{17}O chemical shifts and Mo–O bond distances ranging from 1.6 to 2.4 Å, but over the narrower range of terminal Mo–O (oxo) distances, 1.6–1.9 Å, Wentworth and Miller[22] have proposed a linear correlation between chemical shift and Mo–O bond distance. According to the Wentworth–Miller correlation, the ^{17}O chemical shift found for $MoO_2(O\text{-}i\text{-}Pr)_2(bpy)$ leads to a predicted Mo–O (oxo) distance of 1.71 Å, which agrees well with the average distance found in the solid-state structure.

It should also be noted that the ^{17}O chemical shifts for $MoO_2(OR)_2(py)_2$ and $MoO_2(OR)_2(bpy)$ compounds are smaller than those of other octahedral *cis*-$MoO_2{}^{2+}$-containing compounds, e.g. $MoO_2(acac)_2$ (1025 ppm) and $MoO_2(S_2CNEt_2)_2$ (975 ppm).[22] This implies somewhat less oxo–molybdenum π bonding in $MoO_2(OR)_2(bpy)$ compounds than the maximum π-bond order of 1.5, which is possible for a *cis*-$MoO_2{}^{2+}$-containing compound. According to a Miller–Wentworth plot of π-bond order vs. ^{17}O chemical shift, a π-bond order of 1.37 per Mo–O (oxo) bond is determined for $MoO_2(OR)_2(py)_2$ and $MoO_2(OR)_2(bpy)$ compounds. Apparently, the alkoxy groups are also competing as π-donor ligands. This is supported by considerations of oxo and alkoxy Mo–O bond distances discussed later.

Solid-State Molecular Structure of $MoO_2(O\text{-}i\text{-}Pr)_2(bpy)$. An ORTEP view of the $MoO_2(O\text{-}i\text{-}Pr)_2(bpy)$ molecule is shown in Figure 1. Atomic coordinates are given in Table V. Selected bond distances and bond angles are reported in Tables VI and VII. Anisotropic thermal parameters and complete listings of bond distances and angles are available in the supplementary material.

The molecule has virtual C_{2v} symmetry. The geometry about molybdenum is a distorted-octahedral one. All of the

---

(20) Kidd, R. G. *Can. J. Chem.* **1967**, *45*, 605.
(21) Freeman, M. A.; Schultz, F. A.; Reilley, C. N. *Inorg. Chem.* **1982**, *21*, 567.
(22) Miller, K. F.; Wentworth, R. A. D. *Inorg. Chem.* **1979**, *18*, 984.
(23) Haymore, B. L.; Nugent, W. A. *Coord. Chem. Rev.* **1980**, *31*, 123.

Table V. Fractional Coordinates for the $MoO_2(O\text{-}i\text{-}Pr)_2(bpy)_2$ Molecule

atom	10^4x	10^4y	10^4z
Mo(1)	5167 (1)	8152 (1)	3020.7 (5)
N(2)	5882 (6)	10221 (10)	2537 (4)
C(3)	5296 (8)	11319 (13)	2419 (6)
C(4)	5694 (8)	12545 (14)	2142 (6)
C(5)	6747 (8)	12696 (12)	2005 (5)
C(6)	7372 (8)	11527 (12)	2133 (5)
C(7)	6886 (7)	10352 (11)	2409 (5)
C(8)	7474 (7)	9084 (12)	2559 (5)
C(9)	8502 (7)	9073 (12)	2464 (6)
C(10)	8991 (7)	7865 (13)	2635 (6)
C(11)	8437 (8)	6675 (13)	2860 (5)
C(12)	7398 (7)	6774 (12)	2944 (5)
N(13)	6934 (6)	7959 (9)	2804 (4)
O(14)	5068 (5)	6524 (9)	3333 (4)
O(15)	3989 (5)	8743 (9)	2999 (4)
O(16)	5132 (5)	9921 (8)	3957 (3)
C(17)	4922 (8)	11723 (12)	4332 (6)
C(18)	3938 (8)	12138 (14)	5051 (6)
C(19)	5833 (9)	12356 (15)	4563 (7)
O(20)	5743 (5)	6725 (8)	1935 (4)
C(21)	5392 (9)	6747 (14)	1338 (6)
C(22)	4960 (9)	5106 (14)	1053 (6)
C(23)	6286 (11)	6959 (18)	709 (7)
Mo(1)′	743 (1)	2019 (1)	2208.2 (5)
N(2)′	1388 (5)	4351 (9)	1947 (4)
C(3)′	1138 (7)	4851 (12)	1445 (5)
C(4)′	1475 (7)	6311 (12)	1319 (5)
C(5)′	2066 (7)	7260 (12)	1707 (5)
C(6)′	2340 (7)	6725 (12)	2227 (5)
C(7)′	1991 (6)	5264 (11)	2327 (5)
C(8)′	2252 (7)	4564 (11)	2834 (5)
C(9)′	2900 (7)	5315 (13)	3231 (6)
C(10)′	3141 (7)	4542 (13)	3688 (5)
C(11)	2722 (7)	3065 (13)	3719 (6)
C(12)′	2108 (7)	2387 (13)	3300 (6)
N(13)′	1861 (6)	3128 (9)	2868 (4)
O(14)′	512 (5)	557 (8)	2624 (4)
O(15)′	9 (5)	1765 (8)	1634 (4)
O(16)′	−155 (5)	3935 (8)	3083 (3)
C(17)′	−552 (7)	4069 (12)	3875 (5)
C(18)′	−420 (9)	5844 (13)	4383 (6)
C(19)′	−1663 (8)	3771 (14)	4050 (6)
O(20)′	2047 (5)	823 (8)	1438 (3)
C(21)′	2662 (11)	789 (16)	715 (8)
C(22)′	3742 (40)	926 (67)	720 (28)
C(23)′	2371 (35)	9014 (54)	141 (25)
C(22A)′	3862 (32)	945 (54)	989 (22)
C(23A)′	3645 (25)	152 (42)	423 (19)
C(22B)′	2956 (28)	−697 (43)	135 (19)
C(23B)′	2082 (30)	−540 (49)	104 (23)
C(1)″	343 (9)	−139 (15)	4346 (7)
C(2)″	1490 (12)	−607 (19)	4995 (9)
C(3)″	445 (18)	−262 (31)	5030 (14)
C(4)″	1361 (18)	−530 (29)	4307 (13)
C(5)″	−581 (21)	215 (33)	4371 (15)
C(6)″	9512 (24)	6916 (39)	295 (17)
C(7)″	8829 (22)	5561 (36)	730 (15)
C(8)″	10755 (20)	6242 (34)	−501 (15)
C(9)″	9275 (21)	8189 (37)	352 (15)
C(10)″	716 (23)	3863 (45)	−445 (17)
C(11)″	6 (27)	6486 (42)	−52 (19)
C(12)″	9391 (22)	4883 (42)	406 (16)

Table VI. Selected Bond Distances (Å) for the $MoO_2(O\text{-}i\text{-}Pr)_2(bpy)$ Molecule

Mo(1)–O(14)	1.689 (7)	O(20)–C(21)	1.432 (11)
Mo(1)–O(15)	1.723 (6)	N(2)–C(3)	1.352 (12)
Mo(1)–O(16)	1.914 (6)	N(2)–C(7)	1.350 (12)
Mo(1)–O(20)	1.945 (6)	N(13)–C(8)	1.351 (12)
Mo(1)–N(2)	2.367 (8)	N(13)–C(12)	1.336 (11)
Mo(1)–N(13)	2.346 (8)	C–C (bpy)	1.40 (1) av
O(16)–C(17)	1.405 (11)	C–C (isopropyl)	1.53 (1) av

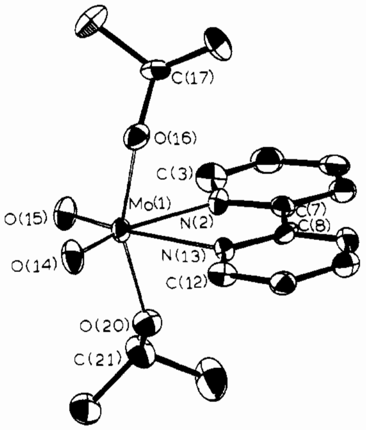

Figure 1. ORTEP view of the $MoO_2(O\text{-}i\text{-}Pr)_2(bpy)$ molecule giving the atom-numbering scheme used in the tables.

Table VII. Selected Bond Angles (deg) for the $MoO_2(O\text{-}i\text{-}Pr)_2(bpy)$ Molecule

O(14)–Mo(1)–O(15)	108.0 (3)	O(16)–Mo(1)–N(2)	81.0 (3)
O(14)–Mo(1)–O(16)	96.6 (3)	O(16)–Mo(1)–N(13)	81.0 (3)
O(14)–Mo(1)–O(20)	96.7 (3)	O(20)–Mo(1)–N(2)	79.9 (3)
O(14)–Mo(1)–N(2)	160.9 (3)	O(20)–Mo(1)–N(13)	78.3 (3)
O(14)–Mo(1)–N(13)	91.7 (3)	N(2)–Mo(1)–N(13)	69.2 (3)
O(15)–Mo(1)–O(16)	100.4 (3)	Mo(1)–O(16)–C(17)	140.0 (6)
O(15)–Mo(1)–O(20)	94.7 (3)	Mo(1)–O(20)–C(21)	128.2 (6)
O(15)–Mo(1)–N(2)	91.0 (3)	Mo–O–C_α (isopropoxide)	130.0 (10) av
O(15)–Mo(1)–N(13)	159.8 (3)	C_β–C_α–C_β (isopropoxide)	109.0 (10) av
O(16)–Mo(1)–O(20)	155.7 (3)	C–C–C (bpy)	120.0 (10) av

distortions are easily understood. The oxo–Mo–oxo angle of 108° arises from the repulsive interactions of the cis multiple bonds. These forces also operate to bend the mutually trans O–*i*-Pr ligands away from the O–O edge of the octahedron. The planar bpy ligand, with its small bite, 69°, easily accommodates this distortion. The Mo–O (oxo) distance, 1.71 Å (averaged), is slightly longer than those typically found for terminal *cis*-MoO_2^{2+} compounds, 1.68 Å, which is consistent with the view, previously expressed as a result of the ^{17}O chemical shift data, that the maximum Mo–O (oxo) π-bond order is not attained because of RO-to-Mo π bonding. The Mo–O (alkoxy) distance, 1.93 Å (averaged), is sufficiently short to be suggestive of some alkoxy-to-molybdenum π bonding.[24] It is, however, notably longer than the Mo–OR (terminal) distance, 1.81 Å (averaged), found in $Mo_2(O\text{-}i\text{-}Pr)_6X_4$ compounds (X = Cl, Br),[2] where RO-to-Mo π bonding does not have to compete with other strong π-donor ligands. The Mo–N (bpy) distance, 2.34 Å (averaged), is long, presumably because of the high trans influence of the trans oxo ligands.[25] The C–C and C–N distances of the bpy ligand are normal, and an interesting comparison with the short Mo–N and distorted bpy C–C and C–N distances found in the $Mo(O\text{-}i\text{-}Pr)_2(bpy)_2$ molecule will be made elsewhere.[26]

The ability of the $MoO_2(O\text{-}i\text{-}Pr)_2$ unit to coordinate bpy leads to the expectation that $MoO_2(OR)_2$ compounds, where R = *i*-Pr and $CH_2\text{-}t\text{-}Bu$, are polymeric in the solid state.

$MoO(OR)_4$ Compounds. $MoO(O\text{-}t\text{-}Bu)_4$ and $MoO(O\text{-}i\text{-}Pr)_4$ are yellow liquids that can be vacuum distilled. $MoO(OCH_2\text{-}t\text{-}Bu)_4$ is a yellow solid that can be sublimed under vacuum and crystallized from toluene or hexane solutions. All three compounds are stable under a dry oxygen or nitrogen atmosphere but quickly decompose to give blue molybdenum oxides when exposed to moisture. The ^{17}O and ^{1}H NMR

---

(24) Chisholm, M. H. *Polyhedron*, in press.

(25) Appleton, T. G.; Clark, H. C.; Manzer, L. M. *Coord. Chem. Rev.* **1973**, *10*, 335.

(26) Chisholm, M. H.; Huffman, J. C.; Rothwell, I. P.; Woodruff, W. H.; Bradley, P. G.; Kress, N. *J. Am. Chem. Soc.* **1981**, *103*, 4945.

Table VIII. Significant Ions in the Mass Spectrum of the New Oxo-Alkoxy Compounds

compd	temp, °C	m/e^a
$MoO_2(O\text{-}t\text{-}Bu)_2$	56	261 (22), 205 (100)
$MoO_2(O\text{-}t\text{-}Bu)_2(bpy)$	69	261 (100), 205 (20)
$MoO_2(O\text{-}i\text{-}Pr)_2(bpy)$	74	233 (71), 191 (100)
$Mo^{18}O_2(O\text{-}i\text{-}Pr)_2(bpy)$	60	237 (100), 195 (7.7)
$MoO_2(O\text{-}i\text{-}Pr\text{-}d_6)_2(bpy)^b$	102	242 (73), 195 (100)
$MoO_2(OCH_2\text{-}t\text{-}Bu)_2(bpy)$	75	274 (53), 256 (100)
$MoO(O\text{-}t\text{-}Bu)_4$	45	333 (10), 277 (5.1), 221 (100), 165 (80)
$MoO(O\text{-}i\text{-}Pr)_4$	58	291 (14), 249 (9.3), 207 (47), 165 (100)
$MoO(OCH_2\text{-}t\text{-}Bu)_4$	27	375 (100)

[a] All ions are based on ^{98}Mo. Parenthetical value is the relative percent intensity. Base peak = 100%. [b] $(O\text{-}i\text{-}Pr\text{-}d_6)$ represents $[OCH(CD_3)_2]$.

spectra indicate only one type of oxo ligand and one type of OR ligand, respectively. The ^{17}O chemical shift values are within the range expected for terminal oxo groups bonded to Mo(6+).[19] Cryoscopic molecular weight determinations in benzene on $MoO(O\text{-}i\text{-}Pr)_4$ and $MoO(OCH_2\text{-}t\text{-}Bu)_4$ show that they are predominantly monomeric in solution with observed (calculated) molecular weights of 410 ± 30 (348) and 499 ± 50 (460), respectively. Since the steric bulk of the alkoxide ligands is in the order $t\text{-}BuO > i\text{-}PrO > OCH_2\text{-}t\text{-}Bu$,[27] the compound $MoO(O\text{-}t\text{-}Bu)_4$ is almost certainly a monomer. Since the observed molecular weights are slightly higher than that of the monomer, it is likely that there is rapid monomer $\rightleftharpoons$ dimer equilibrium in solution with the position of the equilibrium favoring the monomer. However, in the solid state, weak association through RO bridge formation could lead to octahedral coordination for molybdenum as shown in III. The infrared spectra (Nujol mulls) show terminal Mo=O stretches at 967, 951, and 915 cm^{-1} for R = t-Bu, i-Pr, and $CH_2\text{-}t\text{-}Bu$, respectively.

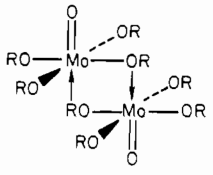

III

The related compound $MoO(OC(CF_3)_3)_4$ has been prepared[28] from the reaction between $MoOCl_4$ and $NaOC(CF_3)_3$ in CH_2Cl_2 solvent. The molecular structure of this volatile yellow solid showed the central MoO_5 unit is a distorted square-based pyramid with the oxo ligand in the apical position. A similar geometry is expected for $MoO(O\text{-}t\text{-}Bu)_4$. The possibility that the $MoO(OR)_4$ compounds, where R = i-Pr and $CH_2\text{-}t\text{-}Bu$, are dimers cannot be overlooked, however, and the molecular structure of $Mo_6O_{10}(O\text{-}i\text{-}Pr)_{12}$, discussed later, may be viewed as the sum of two $MoO(O\text{-}i\text{-}Pr)_4$ molecules associated to two $Mo_2O_4(O\text{-}i\text{-}Pr)_2$ units. The lower values of ν(Mo=O) for R = i-Pr (951 cm^{-1}) and R = $CH_2\text{-}t\text{-}Bu$ (915 cm^{-1}) relative to ν(Mo=O) for R = t-Bu (967 cm^{-1}) may well reflect the formation of weak RO→Mo bonds trans to Mo=O bonds in the former compounds.

Mass Spectra of Mo(6+) Oxo Alkoxides: A General Scheme. The mass spectra of all the new Mo(6+) oxo alkoxides were examined by the method of direct insertion using electron impact ionization. None of the new compounds showed a molecular ion. The bpy and pyridine adducts lose the Lewis base ligands in the vapor state. Hence, $MoO_2(O\text{-}t\text{-}Bu)_2$, $MoO_2(O\text{-}t\text{-}Bu)_2(py)_2$, and $MoO_2(O\text{-}t\text{-}Bu)_2(bpy)$ all show identical fragmentation patterns for the metal-containing ions. The ions of highest mass are shown in Table VIII.

Scheme I

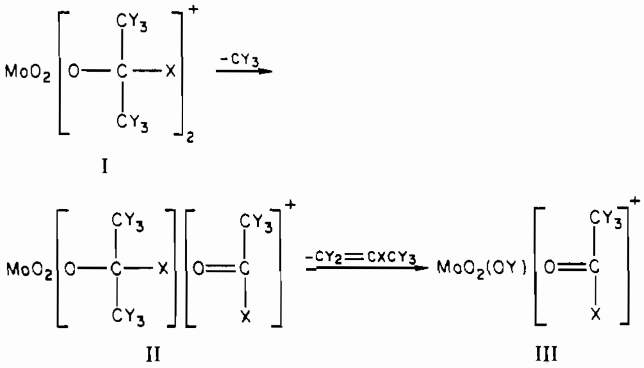

compd	X	Y	m/e		
			I^a	II	III
$MoO_2(O\text{-}t\text{-}Bu)_2$	Me	H	276	261	205
$MoO_2(O\text{-}i\text{-}Pr)_2(bpy)$	H	H	248	233	191
$Mo^{18}O_2(O\text{-}i\text{-}Pr)_2(bpy)$	H	H	252	237	195
$MoO_2(O\text{-}i\text{-}Pr\text{-}d_6)_2(bpy)$	H	D	260	242	195

[a] No molecular ions are observed in the mass spectrum. All ions are based on ^{98}Mo.

$MoO_2(O\text{-}i\text{-}Pr)_2(bpy)$ was prepared by using a variety of isotopic labels in order to assist in determining the fragmentation pattern. The mass spectrum of $Mo^{18}O_2(O\text{-}i\text{-}Pr)_2(bpy)$ is similar to that of $MoO_2(O\text{-}i\text{-}Pr)_2(bpy)$: all the metal-containing ions show an increase of 4 mass units. The oxo ligands are thus shown to be derived from molecular oxygen, and oxo groups are not eliminated during mass spectral fragmentation. The fragmentation is entirely due to the alkoxide ligands. For protio compounds, the ion of highest mass corresponds to M − 15, and deuterio compounds show M − 18, corresponding to loss of CH_3 and CD_3, respectively. This is then followed by a loss of alkene by abstraction of H/D from a carbon atom β to the alkoxide oxygen atom. This type of fragmentation has been seen before for other metal isopropoxides[29] and is summarized in Scheme I, which shows the results of the pertinent labeling experiments.

$MoO_2(O\text{-}t\text{-}Bu)_2(bpy)$ follows the same pattern: initial loss of methyl from a *tert*-butoxy group is followed by elimination of isobutylene from the other. A similar fragmentation pattern is seen for $Cr(O\text{-}t\text{-}Bu)_4$.[30]

The $MoO(OR)_4$ compounds fragment in a manner akin to that previously described for $WO(O\text{-}t\text{-}Bu)_4$.[31] Initial loss of an alkoxide ligand, followed by elimination of alkene, yields the ion fragments in the series $MoO(OR)_4^+ \rightarrow MoO(OR)_3^+ \rightarrow MoO(OH)(OR)_2^+ \rightarrow MoO(OH)_2(OR)^+ \rightarrow MoO(OH)_3^+$.

$Mo_3O(OR)_{10}$ Compounds (R = i-Pr, $CH_2\text{-}t\text{-}Bu$): Solution and Physicochemical Properties. The compounds $Mo_3O(OR)_{10}$, where R = i-Pr and $CH_2\text{-}t\text{-}Bu$, are green crystalline solids that are indefinitely stable under a nitrogen atmosphere and in solution. They slowly react with molecular oxygen to form $MoO_2(OR)_2$ compounds with the elimination of alkoxy radicals, and they hydrolyze in the presence of moisture. They are soluble in aromatic and aliphatic hydrocarbons and methylene chloride but insoluble and unreactive toward pyr-

---

(27) Bradley, D. C.; Mehrotra, R. C.; Gaur, D. P. "Metal Alkoxides"; Academic Press: New York, 1978.

(28) Johnson, D. A.; Taylor, J. C.; Waugh, A. B. *J. Inorg. Nucl. Chem.* **1980**, *42*, 1271.

(29) Oliver, J. G.; Worrall, I. J. *J. Chem. Soc. A* **1970**, 2347.

(30) Alyea, E. C.; Basi, J. S.; Bradley, D. C.; Chisholm, M. H. *J. Chem. Soc. A* **1971**, 772.

(31) Bradley, D. C.; Chisholm, M. H.; Extine, M. W.; Stager, M. E. *Inorg. Chem.* **1977**, *16*, 179.

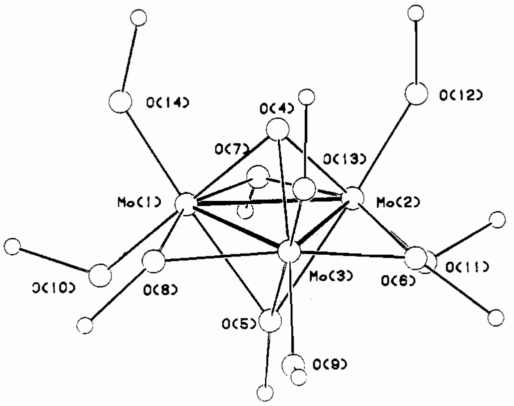

Figure 2. ORTEP view of the central Mo_3O_{11} skeleton found in the $Mo_3O(OR)_{10}$ molecules (R = CH_2-*t*-Bu, *i*-Pr) showing the atom-numbering scheme used in the tables. The oxo ligand is O(4).

idine. The $Mo_3O(OR)_{10}$ compounds decompose at temperatures above 100 °C and could not be sublimed in vacuo. No metal-containing ions were observed in the mass spectrometer.

^1H NMR spectra of $Mo_3O(O\text{-}i\text{-}Pr)_{10}$ compounds are consistent with expectations based upon considerations of the molecular structures found in the solid state that have virtual C_{3v} symmetry. The presence of four types of alkoxy ligands in the ratio 3:3:3:1 shows that bridge–terminal exchange is not rapid on the NMR timescale. The spectra are unaffected by added pyridine, indicating that bridging OR ligands cannot readily be displaced by donor ligands. No signal was observed in the natural-abundance ^{17}O NMR spectrum, and the preparation of $Mo_3{}^{18}O(O\text{-}i\text{-}Pr)_{10}$ did not allow an assignment of $\nu(Mo_3\text{-}\mu_3\text{-}O)$ by a comparison with the ^{16}O infrared spectrum.

A more detailed study of the electronic spectra and electrochemical behavior of these $Mo_3O(OR)_{10}$ compounds is currently under way.

Solid-State and Molecular Structures. Crystals of the neopentoxide were first examined, and while the structure was readily solved, a disorder problem associated with one of the neopentyl ligands (the μ_3-OR ligand), a partial occupancy of a solvent molecule within the unit cell that refined to a 0.33 occupancy factor, and the general rather high thermal vibrations associated with the neopentyl methyl groups all contributed to a rather unsatisfactory characterization. Consequently, the isopropoxide was also examined. Atomic positional parameters are given for $Mo_3O(OCH_2\text{-}t\text{-}Bu)_{10}$ and $Mo_3O(O\text{-}i\text{-}Pr)_{10}$ in Tables IX and X, respectively.

In the space group $P\bar{1}$, there are two independent $Mo_3O(O\text{-}i\text{-}Pr)_{10}$ molecules in the unit cell, differing only slightly with respect to the conformations of the isopropyl groups. A least-squares fit of the $Mo_3O(OC_\alpha)_{10}$ skeletons of the $Mo_3O(O\text{-}i\text{-}Pr)_{10}$ molecules to the $Mo_3O(OC_\alpha)_{10}$ skeleton of the $Mo_3O(OCH_2\text{-}t\text{-}Bu)_{10}$ molecule was performed by fitting the three molybdenum atoms and then calculating the difference in positions of the unmatched atoms. The $Mo_3O(OC_\alpha)_{10}$ skeletons are virtually identical, with no oxygen atom differing by more than 0.21 (1) Å and no C_α differing by more than 0.95 (1) Å. Comparisons of bond distances and bond angles for the central Mo_3O_{11} units of the three crystallographically independent $Mo_3O(OR)_{10}$ molecules are given in Tables XI and XII, respectively. An ORTEP view of the central Mo_3O_{11} skeleton showing the atom-numbering scheme used for the three molecules is given in Figure 2. Tables listing anisotropic thermal parameters and complete listings of bond distances and angles, together with figures showing the atom-numbering schemes, are given in the supplementary material. Two stereoviews of one of the $Mo_3O(O\text{-}i\text{-}Pr)_{10}$ molecules are shown in Figure 3. These oxo alkoxides of molybdenum are members of a now fairly extensive class of triangulo Mo_3-containing

Table IX. Fractional Coordinates for the $Mo_3O(OCH_2\text{-}t\text{-}Bu)_{10}$ Molecule[a]

atom	10^4x	10^4y	10^4z
Mo(1)	5952 (1)	2582 (2)	153 (2)
Mo(2)	6247 (1)	2604 (2)	−1033 (2)
Mo(3)	6373 (1)	1580 (2)	−220 (2)
O(4)	6509 (7)	2609 (15)	−95 (12)
O(5)	5807 (9)	1849 (16)	−654 (17)
O(6)	6496 (7)	1667 (14)	−1240 (12)
O(7)	5876 (8)	3261 (14)	−643 (14)
O(8)	6048 (9)	1659 (16)	646 (14)
O(9)	6264 (8)	568 (14)	−271 (13)
O(10)	5425 (7)	2551 (16)	390 (12)
O(11)	6007 (7)	2602 (17)	−1930 (11)
O(12)	6626 (9)	3233 (17)	−1293 (16)
O(13)	6845 (9)	1387 (15)	144 (16)
O(14)	6086 (9)	3239 (16)	810 (14)
C(15)*	5411 (26)	1809 (46)	−997 (47)
C(16)*	5320 (47)	1059 (87)	−298 (90)
C(17)	5341 (15)	1101 (30)	−1161 (28)
C(18)	5563 (18)	764 (33)	−1680 (31)
C(19)*	5233 (27)	679 (50)	−429 (43)
C(20)*	4872 (27)	993 (55)	−1500 (47)
C(21)*	4999 (32)	618 (55)	−1124 (57)
C(22)*	5059 (31)	1884 (55)	−1502 (52)
C(23)	6539 (13)	1199 (24)	−1855 (22)
C(24)	6963 (16)	1230 (29)	−2148 (26)
C(25)	7007 (15)	1937 (27)	−2497 (26)
C(26)	7245 (14)	1143 (27)	−1531 (23)
C(27)	7022 (19)	582 (37)	−2636 (34)
C(28)	5519 (14)	3551 (27)	−909 (26)
C(29)	5520 (16)	4386 (29)	−877 (28)
C(30)	5842 (15)	4659 (28)	−1261 (27)
C(31)	5144 (14)	4631 (26)	−1239 (24)
C(32)	5508 (12)	4613 (22)	−128 (23)
C(33)	5839 (11)	1154 (21)	1105 (21)
C(34)	5982 (15)	1167 (28)	1867 (24)
C(35)	5755 (17)	561 (31)	2190 (29)
C(36)	5876 (13)	1891 (23)	2199 (22)
C(37)	6408 (17)	1057 (28)	1865 (25)
C(38)	6496 (11)	0 (23)	−10 (20)
C(39)	6314 (12)	−693 (21)	−140 (21)
C(40)	6303 (11)	−862 (19)	−927 (18)
C(41)	5902 (13)	−734 (24)	129 (25)
C(42)	6595 (11)	−1283 (18)	216 (21)
C(43)	5223 (13)	2982 (23)	916 (22)
C(44)	4811 (13)	2732 (25)	1011 (23)
C(45)	4637 (15)	3134 (28)	1581 (26)
C(46)	4783 (13)	1926 (23)	1167 (24)
C(47)	4640 (13)	2808 (25)	276 (26)
C(48)	6122 (12)	3062 (21)	−2504 (21)
C(49)	5884 (13)	2986 (23)	−3127 (22)
C(50)	5956 (14)	2280 (28)	−3423 (23)
C(51)	5456 (16)	3080 (28)	−2963 (27)
C(52)	6046 (20)	3489 (40)	−3683 (34)
C(53)	6973 (13)	3435 (26)	−953 (24)
C(54)	7183 (16)	4083 (29)	−1247 (27)
C(55)	6884 (15)	4728 (28)	−1282 (27)
C(56)	7514 (16)	4153 (27)	−814 (24)
C(57)	7263 (16)	3813 (31)	−2066 (27)
C(58)	7125 (15)	1852 (25)	353 (25)
C(59)	7450 (15)	1440 (26)	662 (23)
C(60)	7763 (21)	1983 (27)	932 (40)
C(61)	7374 (16)	834 (31)	1221 (31)
C(62)	7672 (19)	1160 (35)	57 (32)
C(63)	6444 (17)	3511 (30)	986 (28)
C(64)	6457 (18)	4139 (29)	1582 (27)
C(65)	6865 (26)	4247 (48)	1875 (44)
C(66)	6076 (22)	4419 (42)	1729 (38)
C(67)	6260 (30)	3698 (60)	2380 (54)
Cl(68)[b]	3606 (12)	3455 (22)	495 (18)
Cl(69)[b]	3207 (14)	2726 (27)	1479 (24)

[a] Atoms marked by an asterisk were disordered. [b] The occupancy factor on the Cl atoms refined to an average value of 0.33.

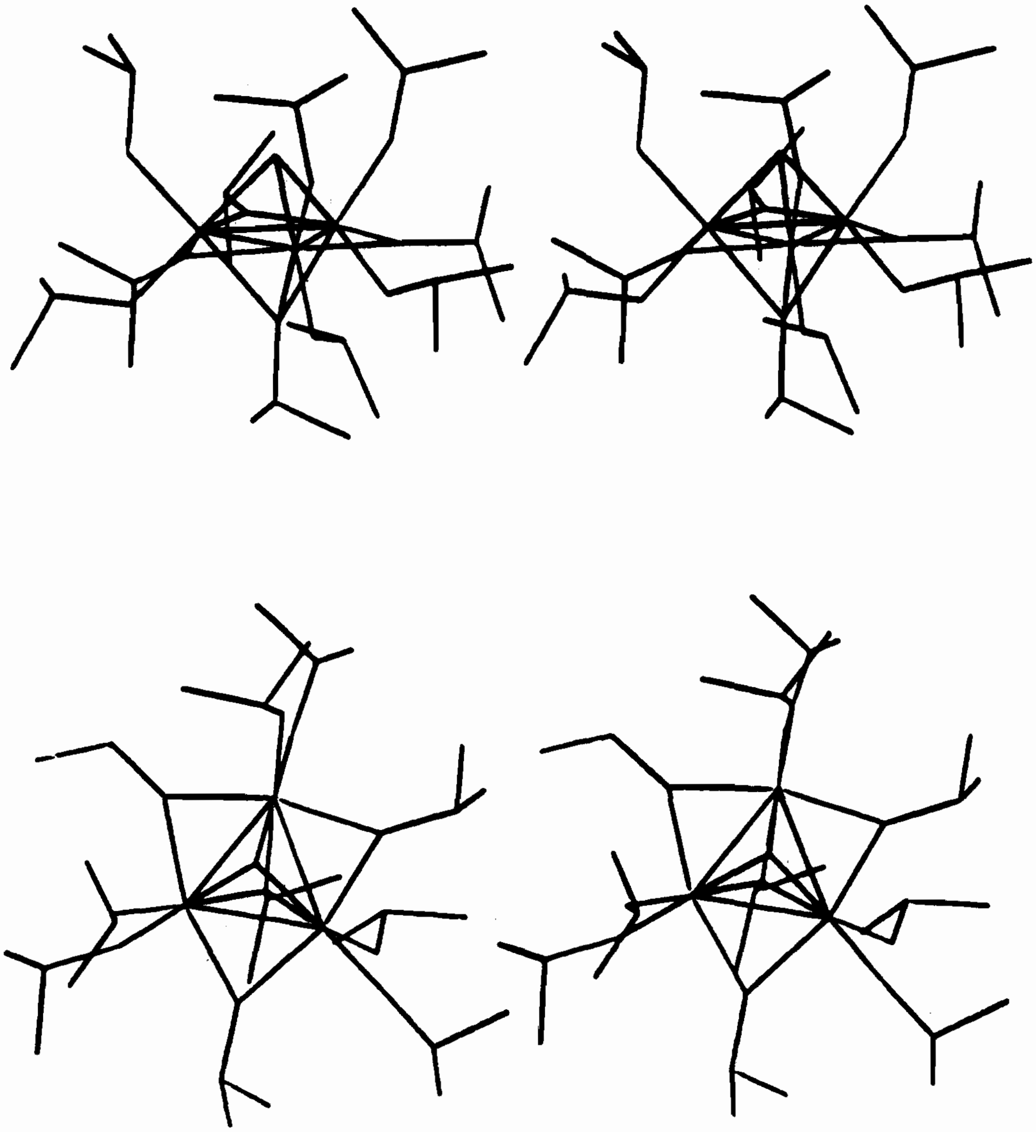

Figure 3. Two stereoviews of one of the two $Mo_3O(O\text{-}i\text{-}Pr)_{10}$ molecules found in the asymmetric unit of the unit cell.

compounds with either one or two capping ligands.[32] The geometry of the oxo alkoxide cluster is, however, different from any previously seen. The most pertinent comparisons are with the oxo-capped clusters $Mo_3O_4(C_2O_4)_3(H_2O)_3^{2+}$ and $Mo_3O_2(O_2CMe)_6(H_2O)_3^{2+}$, which contain central Mo_3O_{13}[33] and Mo_3O_{17}[34] skeletons, respectively. A comparison of the Mo_3O_{11} unit in $Mo_3O(OR)_{10}$ compounds with the Mo_3O_{13} and Mo_3O_{17} skeletons is shown in Figure 4. The Mo_3O_{17} unit allows each molybdenum atom to be seven-coordinate while, in both Mo_3O_{11} and Mo_3O_{13}, the molybdenum atoms are six-coordinate, being in a roughly octahedral environment. The oxalate-containing ion, $Mo_3O_4(C_2O_4)_3(H_2O)_3^{2+}$, has a Mo_3O_{13} unit with only one capping ligand, and essentially the same unit is found in a number of ternary oxides of molybdenum having the formula $MM'Mo_3O_8$, where M and M′ are two cations with charge totalling 4+, e.g. Zn_2 or LiSc.[35-37] One could imagine that the Mo_3O_{11} unit of $Mo_3O(OR)_{10}$ compounds could be converted to the Mo_3O_{13} unit by a Lewis base association reaction involving the addition of a pair of alkoxide

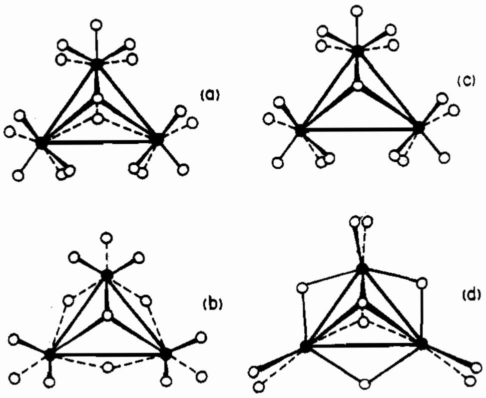

Figure 4. Prototypal representations of the four types of trinuclear cluster structures known for molybdenum and/or tungsten compounds:[53] (a) the bicapped structure found in $[M_3X_2(O_2CR)_6(H_2O)_3]^{n+}$ species; (b) the trigonal M_3O_4 type found in, for example, the Mo(IV) aquo ion; (c) the hemicapped structure found in $[W_3O(O_2CMe)_6(H_2O)_3]ZnBr_4\cdot 8H_2O$; (d) the structure found in $Mo_3O(OR)_{10}$ compounds reported here.

ligands: $Mo_3O(OR)_{10} + 2NaOR \rightarrow Na_2Mo_3O(OR)_{12}$. One might also imagine that a CO_2 insertion reaction,[38] or an

---

[32] Muller, A.; Jostes, R.; Cotton, F. A. *Angew. Chem., Int. Ed. Engl.* **1980**, *19*, 875.

[33] Bino, A.; Cotton, F. A.; Dori, Z. *J. Am. Chem. Soc.* **1978**, *100*, 5252.

[34] Bino, A.; Cotton, F. A.; Dori, Z. *J. Am. Chem. Soc.* **1981**, *103*, 243.

[35] McCarroll, W. H.; Katz, L.; Ward, J. *J. Am. Chem. Soc.* **1957**, *79*, 5410.

[36] Ansell, G. B.; Katz, L. *Acta Crystallogr.* **1966**, *21*, 482.

[37] McCarley, R. E.; Torardi, C. C. *J. Solid State Chem.* **1981**, *7*, 393.

[38] Chisholm, M. H.; Cotton, F. A.; Extine, M. W.; Reichert, W. W. *J. Am. Chem. Soc.* **1978**, *100*, 1727.

Table X. Fractional Coordinates for the $Mo_3O(O\text{-}i\text{-}Pr)_{10}$ Molecules

atom	10^4x	10^4y	10^4z	atom	10^4x	10^4y	10^4z
Mo(1)	2300 (1)	6934 (1)	6254 (1)	Mo(1)′	7204 (1)	6927 (1)	477 (1)
Mo(2)	3648 (1)	7759 (1)	6610 (1)	Mo(2)′	8128 (1)	8165 (1)	1681 (1)
Mo(3)	2788 (1)	8263 (1)	6608 (1)	Mo(3)′	8385 (1)	7143 (1)	1656 (1)
O(4)	7076 (5)	2311 (5)	2074 (8)	O(4)′	2415 (4)	2724 (4)	7515 (8)
O(5)	7097 (5)	2384 (4)	5092 (8)	O(5)′	1740 (4)	2445 (4)	53 (8)
O(6)	6109 (5)	1216 (5)	3242 (9)	O(6)′	971 (4)	1809 (4)	7494 (8)
O(7)	6910 (5)	3322 (4)	3861 (9)	O(7)′	2868 (5)	2170 (5)	−669 (9)
O(8)	8239 (4)	2503 (5)	3709 (8)	O(8)′	2410 (4)	3770 (4)	9442 (8)
O(9)	7375 (5)	1227 (4)	4670 (8)	O(9)′	863 (5)	2990 (5)	9145 (8)
O(10)	8286 (4)	3777 (4)	5333 (9)	O(10)′	3146 (5)	3384 (5)	1455 (8)
O(11)	5658 (5)	2145 (5)	4631 (9)	O(11)′	1378 (5)	1025 (4)	−834 (8)
O(12)	5726 (5)	2162 (5)	1894 (9)	O(12)′	1926 (5)	1295 (4)	6708 (8)
O(13)	7269 (5)	1140 (5)	1905 (9)	O(13)′	1490 (5)	3222 (5)	6816 (8)
O(14)	8192 (5)	3664 (5)	2561 (9)	O(14)′	3725 (5)	3660 (5)	9085 (9)
C(15)	7071 (7)	2409 (7)	6517 (13)	C(15)′	1431 (6)	2367 (6)	1302 (11)
C(16)	7819 (8)	2591 (7)	7190 (13)	C(16)′	1812 (7)	2100 (7)	2217 (13)
C(17)	6482 (8)	1713 (8)	6760 (15)	C(17)′	616 (7)	1856 (7)	1003 (14)
C(18)	5450 (7)	566 (7)	3365 (16)	C(18)′	322 (7)	1297 (7)	6652 (12)
C(19)	5667 (9)	26 (8)	3670 (17)	C(19)′	242 (7)	1585 (7)	5385 (12)
C(20)	4951 (9)	321 (9)	2037 (16)	C(20)′	314 (7)	−1140 (7)	2557 (13)
C(21)	6870 (9)	3957 (8)	4380 (16)	C(21)′	3385 (7)	1941 (7)	−336 (13)
C(22)	6772 (10)	3959 (9)	5882 (16)	C(22)′	3194 (8)	1608 (8)	874 (14)
C(23)	6223 (8)	3934 (8)	3549 (16)	C(23)′	3383 (8)	1435 (8)	8456 (14)
C(24)	8962 (7)	2565 (8)	3808 (14)	C(24)′	2494 (7)	4459 (6)	10014 (13)
C(25)	−692 (8)	2833 (9)	5262 (15)	C(25)′	2151 (8)	4415 (8)	1286 (13)
C(26)	−604 (8)	3073 (8)	2921 (15)	C(26)′	3300 (8)	5014 (7)	10209 (14)
C(27)	2578 (8)	−574 (7)	5489 (14)	C(27)′	347 (7)	3139 (7)	8525 (12)
C(28)	8140 (8)	712 (8)	4053 (15)	C(28)′	655 (7)	3929 (7)	8494 (14)
C(29)	7385 (10)	389 (9)	5907 (15)	C(29)′	−302 (7)	2870 (8)	−733 (15)
C(30)	8957 (7)	4407 (7)	5470 (14)	C(30)′	3841 (8)	3901 (8)	2105 (13)
C(31)	−698 (9)	4619 (8)	6925 (15)	C(31)′	3758 (9)	4271 (9)	3457 (15)
C(32)	1155 (8)	4986 (7)	4951 (15)	C(32)′	4301 (10)	3552 (10)	2406 (21)
C(33)	4966 (9)	2128 (10)	4483 (20)	C(33)′	8720 (7)	−324 (6)	1173 (13)
C(34)	4395 (11)	1481 (16)	3876 (24)	C(34)′	635 (7)	−117 (7)	7722 (13)
C(35)	4808 (12)	2151 (26)	5940 (28)	C(35)′	8876 (8)	9986 (7)	9905 (13)
C(36)	5806 (8)	2182 (7)	506 (13)	C(36)′	1980 (7)	1455 (6)	5398 (11)
C(37)	5533 (8)	2688 (9)	135 (17)	C(37)′	2770 (7)	1752 (6)	5138 (13)
C(38)	5353 (8)	1418 (8)	−285 (14)	C(38)′	8525 (8)	−764 (7)	5606 (13)
C(39)	7189 (8)	1101 (7)	467 (13)	C(39)′	1933 (7)	3447 (7)	5782 (13)
C(40)	3136 (9)	−308 (8)	10168 (15)	C(40)′	1449 (8)	3390 (8)	4566 (13)
C(41)	7911 (9)	1538 (8)	91 (15)	C(41)′	2515 (8)	4212 (7)	6303 (13)
C(42)	8081 (7)	3612 (7)	1143 (13)	C(42)′	4056 (9)	3615 (10)	7927 (19)
C(43)	7572 (9)	3907 (9)	839 (16)	C(43)′	4782 (14)	3707 (17)	−1614 (33)
C(44)	8814 (9)	4024 (8)	657 (14)	C(44)′	4190 (18)	4170 (26)	7281 (36)

acetate for OR exchange reaction, could convert the Mo_3O_{11} unit to the Mo_3O_{17} unit of $Mo_3O_2(OAc)_6(H_2O)_3^{2+}$: $Mo_3O(OR)_{10} + 6CO_2 \rightarrow Mo_3(\mu_3\text{-}O)(\mu_3\text{-}OR)(\mu\text{-}OR)_3(O_2COR)_6$. These possibilities remain to be explored.

The following general observations concerning the $Mo_3O(OR)_{10}$ structures are worthy of note. (1) The average Mo–O (μ_3-OR) distance, 2.19 (3) Å, is considerably longer than the average Mo–O (μ_3-oxo) distance, 2.04 (3) Å, as expected.[24] (2) The Mo–O (μ-OR) distances, 2.03 (3) Å (averaged), are typical of those distances where there is a metal–metal bond.[24] (3) The Mo–O distances to the terminal alkoxide ligands are short, 1.88 (3) Å, and long, 1.95 (3) Å, when they are trans to the capping alkoxide and oxo ligand, respectively. This presumably reflects the relative trans influence[25] oxo > RO. The Mo–Mo distance, 2.53 Å (averaged), is similar to that in $Mo_3O_4(C_2O_4)_3(H_2O)_3^{2+}$, 2.49 Å, and that in $Zn_2Mo_3O_8$, 2.52 Å, and is indicative of Mo–Mo single bonds in these types of triangulo Mo_3^{12+}-containing species. A ground-state molecular orbital configuration for the M–M bonds, $a^2 + e^4$, may be pictured to arise primarily from combinations of molybdenum atomic d_{z^2} and d_{xz} orbitals, where the z axis is defined as a vector from each molybdenum atom to the center of the Mo_3 triangle and the x axis is in the plane of the triangle.

Further studies on these interesting $Mo_3O(OR)_{10}$ compounds are planned.

$Mo_4O_8(O\text{-}i\text{-}Pr)_4(py)_4$. $Mo_4O_8(O\text{-}i\text{-}Pr)_4(py)_4$ is a red crystalline solid that is insoluble in aliphatic and aromatic hydrocarbon solvents. It is stable in the air for short periods of time but slowly hydrolyzes. $Mo_4{}^{18}O_8(O\text{-}i\text{-}Pr)_4(py)_4$ was prepared from the reaction between $Mo_2(O\text{-}i\text{-}Pr)_6$ and $^{18}O_2$ in the presence of pyridine. A comparison of the infrared spectra of the ^{16}O- and ^{18}O-labeled compounds allows the assignment of $\nu(Mo\text{–}^{16}O)$ = 941 and 918 cm^{-1} for terminal oxo groups and $\nu(Mo\text{–}^{16}O)$ = 727 and 655 cm^{-1} for the bridging oxo ligands.

The molecular structure determined from an X-ray study has been previously described as part of a study of M–M bonding in compounds of formula $M_4(\mu_3\text{-}X)_2(\mu\text{-}X)_4X_{10}$.[39] The structure is represented as II and may be viewed as the product from dimerization of I shown earlier.

$Mo_6O_{10}(O\text{-}i\text{-}Pr)_{12}$. Solution and Physicochemical Properties. $Mo_6O_{10}(O\text{-}i\text{-}Pr)_{12}$ is a yellow-orange crystalline solid that is slightly soluble in aromatic solvents and essentially insoluble in aliphatic hydrocarbon solvents. The ^1H NMR spectrum in toluene-d_8 at +16 °C shows broadened resonances for the O-*i*-Pr ligands, but at +75 °C, there are only a sharp septet and doublet. Evidently at +75 °C, there is rapid scrambling of all alkoxide ligands on the NMR time scale. A cryoscopic molecular weight determination in benzene gave mol wt 483 ± 30, which is much lower than that calculated for the hex-

---

(39) Chisholm, M. H.; Folting, K.; Huffman, J. C.; Kirkpatrick, C. C.; Leonelli, J. *J. Am. Chem. Soc.* **1982**, *103*, 6093.

(40) Colton, R.; McCormick, M. J. *Coord. Chem. Rev.* **1980**, *31*, 1.

Table XI. Bond Distances (Å) for the $Mo_3O(OR)_{10}$ Molecules

bond	R = *i*-Pr I	 II	R = CH_2-*t*-Bu
Mo(1)–Mo(2)	2.538 (2)	2.534 (2)	2.523 (5)
Mo(1)–Mo(3)	2.535 (2)	2.528 (2)	2.524 (6)
Mo(2)–Mo(3)	2.539 (2)	2.528 (2)	2.539 (5)
av Mo–Mo	2.534		2.529
Mo(1)–O(4)	2.064 (8)	2.055 (7)	2.036 (25)
Mo(2)–O(4)	2.064 (8)	2.058 (8)	2.039 (24)
Mo(3)–O(4)	2.068 (8)	2.059 (8)	2.026 (30)
av Mo–(μ_3-O)	2.061		2.034
Mo(1)–O(5)	2.173 (8)	2.155 (7)	2.153 (32)
Mo(2)–O(5)	2.172 (8)	2.157 (7)	2.245 (32)
Mo(3)–O(5)	2.165 (7)	2.139 (7)	2.238 (33)
av Mo–(μ_3-OR)	2.160		2.212
Mo(1)–O(7)	2.015 (8)	2.023 (8)	2.025 (28)
Mo(1)–O(8)	2.036 (7)	2.054 (7)	2.024 (30)
Mo(2)–O(6)	2.024 (8)	2.024 (7)	2.026 (26)
Mo(2)–O(7)	2.043 (8)	2.041 (8)	1.965 (28)
Mo(3)–O(6)	2.053 (9)	2.047 (7)	2.027 (24)
Mo(3)–O(8)	2.009 (8)	2.014 (7)	2.040 (28)
av Mo–(μ-OR)	2.032		2.018
Mo(1)–O(14)	1.891 (8)	1.905 (8)	1.842 (30)
Mo(2)–O(12)	1.910 (8)	1.912 (7)	1.868 (32)
Mo(3)–O(13)	1.893 (8)	1.912 (8)	1.857 (31)
av Mo–OR	1.904		1.856
Mo(1)–O(10)	1.952 (7)	1.959 (8)	1.930 (25)
Mo(2)–O(11)	1.953 (8)	1.945 (8)	1.936 (23)
Mo(3)–O(9)	1.950 (8)	1.950 (8)	1.960 (26)
av Mo–OR	1.952		1.942

anuclear formula. Evidently the Mo_6 chain is fragmented in benzene.

Solid-State and Molecular Structure. The molecule $Mo_6O_{10}(O\text{-}i\text{-}Pr)_{12}$ crystallized from toluene in the space group $P\bar{1}$ with one molecule in the unit cell. The molecule thus has a crystallographically imposed center of symmetry. An ORTEP view of the $Mo_6O_{10}(O\text{-}i\text{-}Pr)_{12}$ molecule giving the atom-numbering scheme used in the tables is shown in Figure 5. Atomic positional parameters are given in Table XIII, and selected bond distances and angles are given in Tables XIV and XV, respectively.

The six molybdenum atoms are, to within 0.01 Å, all in the same plane. The metal–metal distances Mo(1)–Mo(2) = Mo(1)′–Mo(2) = 2.585 (1) Å are indicative of localized Mo–Mo single bonds, while the distances Mo(2)–Mo(3) = Mo(2)′–Mo(3)′ = 3.285 (1) Å and Mo(1)–Mo(1)′ = 3.353 (1) Å are typical of nonbonding distances between molybdenum atoms bridged by a pair of OR ligands.[24] The average oxidation state of molybdenum in $Mo_6O_{10}(O\text{-}i\text{-}Pr)_{12}$ is +5.33, and if charge is partitioned by counting a terminal oxo as 2–, a bridging oxo as 1–, a terminal OR as 1–, and a bridging OR as $^1/_2$– per metal, the oxidation states in the chain are Mo(3) = Mo(3)′ = +6 and Mo(2) = Mo(2)′ = Mo(1) = Mo(1)′ = +5. The Mo–Mo distances clearly indicate that the four electrons available for metal–metal bonding are used to form two localized M–M single bonds.

The centrosymmetric $Mo_6O_{10}(O\text{-}i\text{-}Pr)_{12}$ molecule may be viewed as a dimer of $Mo_3O_5(O\text{-}i\text{-}Pr)_6$, brought together through the agency of a pair of RO bridges. The $Mo_3O_5(O\text{-}i\text{-}Pr)_6$ unit may be further broken down into $MoO(O\text{-}i\text{-}Pr)_4$ and $Mo_2O_4(O\text{-}i\text{-}Pr)_2$ units. While the latter is as yet unknown, when supported by alkoxy bridges as in IV, the fused square-based pyramidal units are similar to scores of $Mo_2O_4^{2+}$-containing compounds.

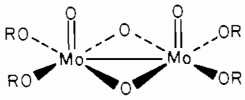

IV

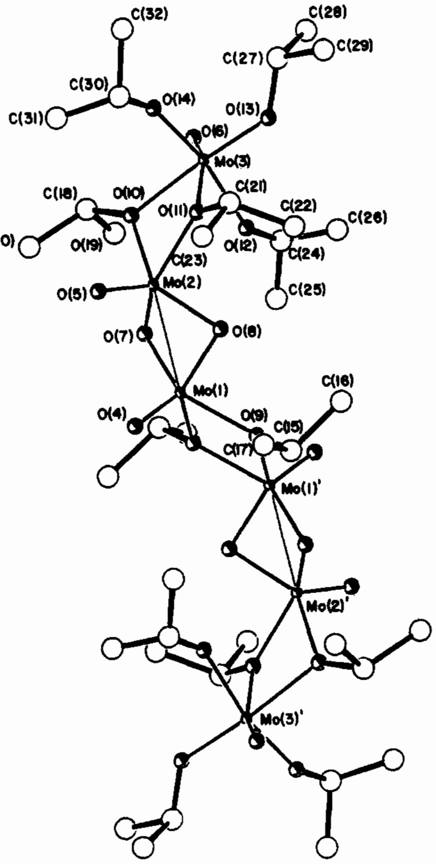

Figure 5. View of the centrosymmetric $Mo_6O_{10}(O\text{-}i\text{-}Pr)_{12}$ molecule giving the atom-numbering scheme used in the tables.

If the Mo–oxo vector is taken as the *z* axis and the M–L bonds are formed using metal s, p_x, p_y, and $d_{x^2-y^2}$ atomic orbitals, the metal–metal bond is easily pictured from the interaction of the d_{xy}–d_{xy} orbitals. Oxygen-to-molybdenum π bonding will use the d_{xz} and d_{yz} orbitals. Some pertinent distances found for the $Mo_2O_4^{2+}$ units in $Mo_6O_{10}(O\text{-}i\text{-}Pr)_{12}$ and $Mo_4O_8(O\text{-}i\text{-}Pr)_4(py)_4$ are compared with those of other compounds in Table XVI.

As with other square-based pyramidal molecules containing a multiple bond in the apical position, the molybdenum atoms lie above the basal plane of the four σ-bonded ligands. The coupling of two $Mo_2O_4(OR)_2$ units in the head-to-tail manner thus produces a zigzag for the four metal atoms. The S curve is completed by attaching the two $MoO(O\text{-}i\text{-}Pr)_4$ units such that one oxygen of an O-*i*-Pr ligand is tucked below the basal plane of its five-coordinate neighbor. The positioning of this group allows for incipient Mo–OR bond formation trans to the oxo–molybdenum bond. Indeed on the basis of the following structural data, we suggest that this one alkoxide ligand is really "semibridging". (1) The terminal Mo(3)–OR distances are all within the range expected,[24] but the Mo(3)–O(12) distance of 1.919 (2) Å is 0.05 Å longer than the others. (2) The Mo(2)- - -O(12) distance is 2.88 (1) Å, too long to be called a bond but much too short for a nonbonding interaction. (3) The Mo(3)–O(12)–C(24) angle is 127.5 (1)°, indicative of sp^2 hybridization at O(12). While the oxygen p_z atomic orbital may π bond to Mo(3), the lone-pair sp^2 orbital, which is contained in the Mo(3)–O(12)–C(24) plane, is directed toward Mo(2). The Mo(2)- - -O(12)–C(24) angle is 83.9 (1)°. If it is agreed that the O(12)- - -Mo(2) interaction is an attractive one, then this can contribute to the folding of the molecule. The Mo(3)–Mo(2)–Mo(1) angle, 134.3 (1)°, is smaller than the Mo(2)–Mo(1)–Mo(1)′ angle, 146.5 (1)°.

The term "semibridging" is now commonly used in metal carbonyl chemistry where semibridging carbonyls may result

Table XII. Bond Angles (deg) for the $Mo_3O(OR)_{10}$ Molecules

	R = *i*-Pr				R = *i*-Pr		
bond	I	II	R = CH_2-*t*-Bu	bond	I	II	R = CH_2-*t*-Bu
Mo(2)-Mo(1)-Mo(3)	60.1 (1)	59.9 (1)	60.4 (2)	O(5)-Mo(2)-O(11)	87.7 (3)	85.9 (3)	89.0 (12)
Mo(2)-Mo(1)-O(4)	52.1 (2)	52.0 (2)	51.8 (7)	O(5)-Mo(2)-O(12)	177.0 (3)	175.8 (3)	176.5 (13)
Mo(2)-Mo(1)-O(5)	54.2 (2)	54.1 (2)	56.7 (9)	O(6)-Mo(2)-O(7)	160.9 (3)	163.0 (3)	157.7 (11)
Mo(2)-Mo(1)-O(7)	51.8 (2)	51.7 (2)	49.7 (8)	O(6)-Mo(2)-O(11)	92.0 (3)	95.9 (3)	90.8 (12)
Mo(2)-Mo(1)-O(8)	110.8 (2)	110.7 (2)	111.9 (8)	O(6)-Mo(2)-O(12)	100.7 (3)	92.3 (3)	101.1 (12)
Mo(2)-Mo(1)-O(10)	127.7 (2)	126.8 (3)	128.3 (7)	O(7)-Mo(2)-O(11)	94.9 (3)	95.4 (3)	92.7 (12)
Mo(2)-Mo(1)-O(14)	123.9 (2)	127.9 (3)	120.5 (9)	O(7)-Mo(2)-O(12)	96.7 (3)	99.3 (3)	100.6 (13)
Mo(3)-Mo(1)-O(4)	52.2 (2)	52.2 (2)	51.4 (8)	O(11)-Mo(2)-O(12)	93.4 (3)	95.0 (3)	94.5 (13)
Mo(3)-Mo(1)-O(5)	54.1 (2)	53.7 (2)	56.5 (9)	Mo(1)-Mo(3)-Mo(2)	60.0 (0)	60.2 (0)	59.8 (1)
Mo(3)-Mo(1)-O(7)	111.6 (2)	111.6 (2)	109.9 (8)	Mo(1)-Mo(3)-O(4)	52.1 (2)	52.0 (2)	51.8 (7)
Mo(3)-Mo(1)-O(8)	50.7 (2)	50.9 (2)	51.9 (8)	Mo(1)-Mo(3)-O(5)	54.4 (2)	54.2 (2)	53.3 (8)
Mo(3)-Mo(1)-O(10)	127.6 (2)	127.7 (2)	128.3 (9)	Mo(1)-Mo(3)-O(6)	110.9 (2)	111.4 (2)	110.2 (8)
Mo(3)-Mo(1)-O(14)	126.8 (2)	125.6 (3)	123.6 (9)	Mo(1)-Mo(3)-O(8)	51.7 (2)	52.3 (2)	51.3 (9)
O(4)-Mo(1)-O(5)	92.3 (3)	91.9 (3)	94.5 (11)	Mo(1)-Mo(3)-O(9)	125.9 (2)	127.6 (2)	129.4 (8)
O(4)-Mo(1)-O(7)	87.3 (3)	83.6 (3)	86.3 (11)	Mo(1)-Mo(3)-O(13)	127.3 (3)	126.3 (2)	125.2 (10)
O(4)-Mo(1)-O(8)	83.9 (3)	85.5 (3)	88.2 (12)	Mo(2)-Mo(3)-O(4)	52.0 (2)	52.1 (2)	51.6 (7)
O(4)-Mo(1)-O(10)	179.7 (3)	178.8 (3)	179.7 (12)	Mo(2)-Mo(3)-O(5)	54.3 (2)	54.3 (2)	55.6 (8)
O(4)-Mo(1)-O(14)	87.1 (3)	88.8 (3)	83.9 (13)	Mo(2)-Mo(3)-O(6)	51.0 (2)	51.2 (2)	51.2 (7)
O(5)-Mo(1)-O(7)	81.1 (3)	85.1 (3)	80.0 (10)	Mo(2)-Mo(3)-O(8)	111.7 (2)	112.4 (2)	110.7 (9)
O(5)-Mo(1)-O(8)	83.3 (3)	81.4 (3)	79.8 (11)	Mo(2)-Mo(3)-O(9)	128.6 (2)	128.0 (2)	133.1 (8)
O(5)-Mo(1)-O(10)	87.4 (3)	87.2 (3)	85.4 (12)	Mo(2)-Mo(3)-O(13)	124.7 (3)	125.9 (2)	123.0 (9)
O(5)-Mo(1)-O(14)	177.7 (3)	177.8 (3)	177.1 (12)	O(4)-Mo(3)-O(5)	92.4 (3)	92.3 (2)	92.2 (10)
O(7)-Mo(1)-O(8)	161.7 (3)	162.4 (3)	158.6 (11)	O(4)-Mo(3)-O(6)	85.7 (3)	84.6 (3)	89.2 (10)
O(7)-Mo(1)-O(10)	92.6 (3)	95.5 (3)	94.0 (12)	O(4)-Mo(3)-O(8)	84.4 (3)	86.4 (3)	88.0 (11)
O(7)-Mo(1)-O(14)	96.7 (3)	97.1 (3)	97.5 (11)	O(4)-Mo(3)-O(9)	177.7 (3)	179.6 (3)	175.3 (11)
O(8)-Mo(1)-O(10)	96.1 (3)	95.3 (3)	91.5 (13)	O(4)-Mo(3)-O(13)	88.0 (3)	88.2 (3)	85.9 (12)
O(8)-Mo(1)-O(14)	98.8 (3)	96.5 (3)	102.5 (11)	O(5)-Mo(3)-O(6)	81.5 (3)	83.4 (3)	79.1 (11)
O(10)-Mo(1)-O(14)	93.3 (3)	92.0 (3)	96.2 (13)	O(5)-Mo(3)-O(8)	84.2 (3)	82.8 (3)	77.5 (12)
Mo(1)-Mo(2)-Mo(3)	59.9 (1)	59.9 (1)	59.8 (2)	O(5)-Mo(3)-O(9)	86.7 (3)	87.5 (3)	91.6 (11)
Mo(1)-Mo(2)-O(4)	52.1 (2)	51.9 (2)	51.7 (7)	O(5)-Mo(3)-O(13)	177.7 (4)	179.5 (3)	178.2 (13)
Mo(1)-Mo(2)-O(5)	54.3 (2)	54.0 (2)	53.3 (8)	O(6)-Mo(3)-O(8)	162.2 (3)	163.2 (3)	156.3 (11)
Mo(1)-Mo(2)-O(6)	111.8 (2)	111.9 (2)	110.3 (7)	O(6)-Mo(3)-O(9)	96.2 (3)	95.7 (3)	94.2 (11)
Mo(1)-Mo(2)-O(7)	50.8 (2)	51.1 (2)	51.8 (8)	O(6)-Mo(3)-O(13)	96.3 (4)	96.3 (3)	100.9 (12)
Mo(1)-Mo(2)-O(11)	128.9 (2)	125.4 (2)	129.1 (8)	O(8)-Mo(3)-O(9)	93.4 (3)	93.2 (3)	90.1 (12)
Mo(1)-Mo(2)-O(12)	123.2 (3)	127.9 (2)	123.8 (10)	O(8)-Mo(3)-O(13)	98.1 (3)	97.6 (3)	102.4 (13)
Mo(3)-Mo(2)-O(4)	52.1 (2)	52.1 (2)	51.1 (8)	O(9)-Mo(3)-O(13)	92.9 (3)	92.0 (3)	90.2 (13)
Mo(3)-Mo(2)-O(5)	54.0 (2)	53.6 (2)	55.4 (8)	Mo(1)-O(4)-Mo(2)	75.9 (3)	76.1 (3)	76.5 (9)
Mo(3)-Mo(2)-O(6)	52.0 (2)	52.0 (2)	51.2 (7)	Mo(1)-O(4)-Mo(3)	75.7 (3)	75.8 (3)	76.8 (10)
Mo(3)-Mo(2)-O(7)	110.5 (2)	111.0 (2)	111.4 (8)	Mo(2)-O(4)-Mo(3)	75.8 (3)	75.7 (3)	77.3 (10)
Mo(3)-Mo(2)-O(11)	126.9 (3)	126.9 (2)	129.1 (10)	Mo(1)-O(5)-Mo(2)	71.5 (2)	72.0 (2)	70.0 (10)
Mo(3)-Mo(2)-O(12)	126.9 (3)	123.2 (2)	121.9 (10)	Mo(1)-O(5)-Mo(3)	71.5 (2)	72.1 (2)	70.2 (10)
O(4)-Mo(2)-O(5)	92.3 (3)	91.8 (3)	91.7 (12)	Mo(2)-O(6)-Mo(3)	77.1 (3)	76.8 (3)	77.6 (9)
O(4)-Mo(2)-O(6)	86.5 (3)	85.2 (3)	88.9 (11)	Mo(1)-O(7)-Mo(2)	77.4 (3)	77.2 (3)	78.4 (10)
O(4)-Mo(2)-O(7)	86.5 (3)	83.1 (3)	87.8 (11)	Mo(1)-O(8)-Mo(3)	77.6 (3)	76.8 (3)	76.8 (10)
O(4)-Mo(2)-O(11)	178.5 (3)	177.3 (3)	179.2 (11)	Mo-O-C_α (alkoxide)	129.0 (10) (av)		129.0 (10) (av)
O(4)-Mo(2)-O(12)	86.7 (3)	87.4 (3)	84.8 (13)	O-C_α-C_β (alkoxide)	108.9 (11) (av)		112.0 (40) (av)
O(5)-Mo(2)-O(6)	82.0 (3)	83.5 (3)	79.0 (11)	C_β-C_α-C_β (alkoxide)	110.8 (13) (av)		109.0 (51) (av)
O(5)-Mo(2)-O(7)	80.5 (3)	84.7 (3)	79.1 (10)				

from either electronic[41,42] or steric factors.[43] Aside from the obvious difference that CO is a π-acceptor and RO is a π-donor ligand, the ligands share a number of common features including their abilities to act as bridging ligands (μ and μ_3) and to support fluxional processes in solution, whereby bridging and terminal groups are exchanged rapidly on the NMR time scale. Though it is possible to envisage that the semibridging OR group is a result of steric factors, we feel it is more likely that the origin is electronic in nature. The five-coordinate Mo(5+) atoms can readily increase their coordination number to 6 by ligation in the position trans to the oxo group. This is seen in the reaction of $Mo_6O_{10}(O\text{-}i\text{-}Pr)_{12}$ with pyridine.

Concluding Remarks. At the outset of this project, one of us had the idea that the addition of molecular oxygen to $Mo_2(OR)_6$ (M≡M) compounds would lead to a series of $Mo_2O_2(OR)_6$ (M–M) compounds. It is easy to envisage one of two structures for compounds of this formula where a d^1–d^1 interaction leads to a metal–metal single bond. These are shown in V and VI.

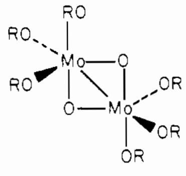

V

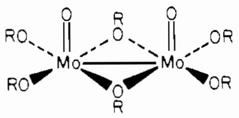

VI

In V, the Mo_2O_8 skeleton is formed by the fusing of two trigonal-bipyramidal units that share a common equatorial–axial edge. This type of structure has been found in a number of molybdenum and tungsten compounds recently, including $[Mo(NAr)(\mu\text{-}NAr)(OR)_2]_2$,[4] $[Mo(NO)(OR)_2(\mu\text{-}OR)]_2$,[44] and $[W(CMe)(O\text{-}t\text{-}Bu)_2(\mu\text{-}O\text{-}t\text{-}Bu)]_2$,[45] which have no M–M bonds, $[W(N_2CAr_2)(\mu\text{-}N_2CAr_2)(O\text{-}t\text{-}Bu)_2]$,[46] which has a

---

(41) Cotton, F. A.; Troup, J. M. *J. Am. Chem. Soc.* **1974**, *96*, 1233.

(42) Cotton, F. A.; Frenz, B. A.; Kruczynski, L. *J. Am. Chem. Soc.* **1973**, *95*, 951.

(43) Bailey, W. I., Jr.; Chisholm, M. H.; Cotton, F. A.; Rankel, L. *J. Am. Chem. Soc.* **1978**, *100*, 5764.

(44) Chisholm, M. H.; Cotton, F. A.; Extine, M. W.; Kelly, R. L. *J. Am. Chem. Soc.* **1978**, *100*, 3354.

(45) Chisholm, M. H.; Hoffman, D. M.; Huffman, J. C. *Inorg. Chem.* **1983**, *22*, 2903.

(46) Chisholm, M. H.; Huffman, J. C.; Ratermann, A. R. *Inorg. Chem.*, in press.

Table XIII. Fractional Coordinates for the $Mo_6O_{10}(O\text{-}i\text{-}Pr)_{12}$ Molecule

atom	10^4x	10^4y	10^4z
Mo(1)	1285.4 (2)	104.2 (3)	−124.9 (3)
Mo(2)	2776.6 (2)	−1044.0 (3)	−1053.6 (3)
Mo(3)	2878.3 (2)	−3886.8 (3)	−2919.9 (3)
O(4)	1897 (2)	1560 (2)	656 (3)
O(5)	3811 (2)	102 (2)	−527 (3)
O(6)	2425 (2)	−4552 (2)	−4658 (3)
O(7)	1723 (2)	9518 (2)	7983 (2)
O(8)	1935 (2)	−1041 (2)	546 (2)
O(9)	−88 (2)	191 (2)	−1148 (2)
O(10)	3086 (2)	−2044 (2)	−3053 (2)
O(11)	3323 (2)	−2541 (2)	−797 (2)
O(12)	1582 (2)	−3505 (2)	−2230 (3)
O(13)	2821 (2)	−5233 (2)	−2193 (3)
O(14)	4301 (2)	−3763 (2)	−3129 (3)
C(15)	−160 (3)	424 (4)	−2556 (4)
C(16)	−13 (4)	1782 (5)	−2328 (5)
C(17)	−1117 (4)	−345 (4)	−3459 (5)
C(18)	3121 (3)	−1741 (3)	−4410 (4)
C(19)	2043 (3)	−2031 (4)	−5174 (4)
C(20)	3629 (3)	9592 (4)	5860 (5)
C(21)	3510 (3)	−2893 (3)	495 (4)
C(22)	2519 (3)	−3539 (4)	945 (4)
C(23)	4065 (3)	−1766 (4)	1671 (4)
C(24)	547 (3)	−4068 (4)	−2897 (4)
C(25)	9870 (4)	6875 (5)	7355 (9)
C(26)	152 (5)	−5113 (6)	−2327 (10)
C(27)	3328 (3)	−6280 (4)	−2573 (5)
C(28)	2669 (4)	−7252 (4)	−3843 (5)
C(29)	3445 (4)	−6718 (5)	−1270 (6)
C(30)	5313 (3)	−3166 (4)	−2432 (4)
C(31)	5664 (3)	−1997 (4)	−2848 (6)
C(32)	6040 (4)	−4076 (5)	−2843 (6)

Table XIV. Selected Bond Distances (Å) for the Centrosymmetric $Mo_6O_{10}(O\text{-}i\text{-}Pr)_{12}$ Molecule

Mo(1)–Mo(2)	2.585 (1)	Mo(3)–O(6)	1.691 (2)
Mo(1)–O(4)	1.673 (2)	Mo(3)–O(10)	2.128 (2)
Mo(1)–O(7)	1.921 (2)	Mo(3)–O(11)	2.197 (2)
Mo(1)–O(8)	1.926 (2)	Mo(3)–O(12)	1.919 (2)
Mo(1)–O(9)	2.058 (2)	Mo(3)–O(13)	1.806 (2)
Mo(2)–O(5)	1.671 (2)	Mo(3)–O(14)	1.865 (2)
Mo(2)–O(7)	1.939 (2)	Mo(2)–Mo(3)	3.285 (1)
Mo(2)–O(8)	1.939 (2)	Mo(1)–Mo(1)′	3.353 (1)
Mo(2)–O(10)	2.057 (2)	O–C_α (isopropoxide)	1.45 (1) (av)
Mo(2)–O(11)	2.044 (2)	C_α–C_β (isopropoxide)	1.51 (1) (av)
Mo(2)–O(12)	2.880 (2)	C–H (isopropoxide)	0.97 (5) (av)

single W–W bond, and $Mo_2(O\text{-}i\text{-}Pr)_8$[12] and $Mo_2(\mu\text{-}S)_2(S\text{-}t\text{-}Bu)_4(HNMe_2)_2$,[47] which have double bonds. By defining the z axis to be coincident with the O–Mo–O axial ligands in V and the x axis to be coincident with the Mo–O equatorial bridge, the d^1–d^1 metal–metal single bond would arise from interaction of d_{xz}–d_{xz} Mo atomic orbitals.

In VI, which has two molybdenum atoms in a local square-based pyramidal environment sharing a common basal edge, it is also easy to picture the formation of a M–M σ bond. By defining the z axis to be coincident with the apical Mo–O(oxo) bond, the d_{xz} and d_{yz} Mo atomic orbitals will be used in Mo–O (oxo) π bonding. One of the orbitals, d_{xy} or $d_{x^2-y^2}$, will be used in forming σ bonds to the RO ligands in the basal plane, and the other, which is not used in metal–ligand bonding, can form a M–M σ bond.

The reaction between $Mo_2(OR)_6$ compounds and O_2 does not lead to the isolation of stable compounds of this formula, however. Whether this is because of kinetic factors, that is to say a reactive intermediate $[Mo(OR)_6O_2]^*$ proceeds directly to $O_2Mo(OR)_2$ and $Mo(OR)_4$ by an asymmetric transition state, or because compounds of types V and VI are formed

Table XV. Selected Bond Angles (deg) for the Centrosymmetric $Mo_6O_{10}(O\text{-}i\text{-}Pr)_{12}$ Molecule

Mo(2)–Mo(1)–O(4)	103.7 (1)	O(6)–Mo(3)–O(10)	94.9 (1)
Mo(2)–Mo(1)–O(7)	48.3 (1)	O(6)–Mo(3)–O(11)	162.8 (1)
Mo(2)–Mo(1)–O(8)	48.2 (1)	O(6)–Mo(3)–O(12)	96.6 (1)
Mo(2)–Mo(1)–O(9)	131.2 (1)	O(6)–Mo(3)–O(13)	103.2 (1)
O(4)–Mo(1)–O(7)	109.9 (1)	O(6)–Mo(3)–O(14)	98.9 (1)
O(4)–Mo(1)–O(8)	110.8 (1)	O(10)–Mo(3)–O(11)	68.9 (1)
O(4)–Mo(1)–O(9)	104.8 (1)	O(10)–Mo(3)–O(12)	82.0 (1)
O(7)–Mo(1)–O(8)	92.1 (1)	O(10)–Mo(3)–O(13)	161.8 (1)
O(7)–Mo(1)–O(9)	142.7 (1)	O(10)–Mo(3)–O(14)	85.8 (1)
O(8)–Mo(1)–O(9)	140.3 (1)	O(11)–Mo(3)–O(12)	75.7 (1)
O(9)–Mo(1)–O(9)	71.5 (1)	O(11)–Mo(3)–O(13)	92.8 (1)
Mo(1)–Mo(2)–O(5)	101.3 (1)	O(11)–Mo(3)–O(14)	86.4 (1)
Mo(1)–Mo(2)–O(7)	47.7 (1)	O(12)–Mo(3)–O(13)	94.3 (1)
Mo(1)–Mo(2)–O(8)	47.8 (1)	O(12)–Mo(3)–O(14)	161.1 (1)
Mo(1)–Mo(2)–O(10)	133.5 (1)	O(13)–Mo(3)–O(14)	92.9 (1)
Mo(1)–Mo(2)–O(11)	136.3 (1)	Mo(1)–O(7)–Mo(2)	84.1 (1)
O(5)–Mo(2)–O(7)	108.4 (1)	Mo(1)–O(8)–Mo(2)	83.9 (1)
O(5)–Mo(2)–O(8)	109.2 (1)	Mo(1)–O(9)–Mo(1)	108.5 (1)
O(5)–Mo(2)–O(10)	103.8 (1)	Mo(2)–O(10)–Mo(3)	103.4 (1)
O(5)–Mo(2)–O(11)	103.5 (1)	Mo(1)–Mo(2)–Mo(3)	134.3 (1)
O(7)–Mo(2)–O(8)	91.1 (1)	Mo(1)′–Mo(1)–Mo(2)	146.5 (1)
O(7)–Mo(2)–O(10)	87.1 (1)	Mo–O–C_α	130.0 (10)
O(7)–Mo(2)–O(11)	145.8 (1)	(isopropoxide)	(av)
O(8)–Mo(2)–O(10)	145.7 (1)	C_β–C_α–C_β	113.0 (10)
O(8)–Mo(2)–O(11)	89.9 (1)	(isopropoxide)	(av)
O(10)–Mo(2)–O(11)	73.3 (1)	O–C_α–C_β	109.0 (10)
		(isopropoxide)	(av)

Table XVI. Structural Properties for Some Diamagnetic Compounds Containing a Central $Mo_2O_4^{2+}$ Moiety

		d(Mo–O), Å		
compd	d(M–M), Å	terminal	bridge	ref
$Mo_6O_{10}(O\text{-}i\text{-}Pr)_{12}$	2.585 (1)	1.67 (1)	1.93 (1)	this work
$Mo_4O_8(O\text{-}i\text{-}Pr)_4(py)_4$	2.600 (1)	1.68 (1), 1.70 (1)	1.94 (1)	39
$Mo_2O_4(C_2O_4)_2(H_2O)_2^{2-}$	2.541 (2)	1.70 (3)	1.91 (3)	54
$Mo_2O_4(Cys)_2^{2-}$	2.569 (2)	1.71 (2)	1.93 (2)	55
$Mo_2O_4(EtCys)_2$	2.569 (2)	1.71 (2)	1.93 (2)	56

but are unstable with respect to asymmetric cleavage is not known. It is certainly quite possible that a reactive intermediate $Mo_2(OR)_6O_2$ could have the geometry shown in VII,

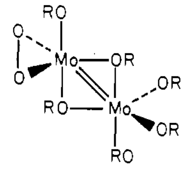

VII

from which oxo group formation and OR bridge cleavage could lead to $O_2Mo(OR)_2$ and $Mo(OR)_4$. Symmetrical intermediates of the types V and VI might never be formed in these reactions.

We did attempt to prepare $[MoO(OR)_3]_n$ compounds from the reaction between $MoOCl_3$ and LiOR (3 equiv), but without success. Only oily products which still contained some chloride were obtained. No $Mo(OR)_4$ or $MoO_2(OR)_4$ compounds were detected. Regrettably, this approach toward the synthesis of species of formula $MoO(OR)_3$ was noninformative.

The new oxo–alkoxy compounds derived from the reactions between $Mo_2(OR)_6$ compounds and molecular oxygen bear witness to the synthetic usefulness of M–M multiple bonds in preparing new mononuclear compounds.[48]

Experimental Section

General Procedures and the preparation of $Mo_2(OR)_6$ compounds have been described.[7] Methylene chloride was distilled from P_2O_5

---

(47) Chisholm, M. H.; Corning, J. C.; Huffman, J. C. *Inorg. Chem.* **1982**, *21*, 286.

(48) Walton, R. A. *ACS Symp. Ser.* **1981**, *No. 155*, 207.

under a nitrogen atmosphere. Pyridine was dried by storing over KOH for 1 week prior to distillation from barium oxide. *tert*-Butyl alcohol was distilled as an azeotrope with dry benzene and was stored over activated molecular sieves prior to use. Isopropyl alcohol was distilled from sodium onto activated molecular sieves. A standard solution of neopentyl alcohol in toluene was prepared by dissolving a known quantity of the solid alcohol in toluene. Additional toluene was added to bring the volume of the solution to a known value, and the solution was stored over molecular sieves.

Analytical data and other spectroscopic and characterization data for the new compounds are reported in Tables I–IV.

^{1}H NMR spectra were recorded on a Varian Associates HR-220 NMR spectrometer in toluene-d_8 with a probe temperature of 16 °C. Natural-abundance ^{17}O NMR spectra were recorded on a Varian Associates XL-100 spectrometer in the Fourier transform mode as previously described.[22] Infrared spectra were recorded on a Perkin-Elmer infrared spectrophotometer. Solid samples were prepared as Nujol mulls between CsI plates. Mass spectra were obtained by the method of direct insertion, courtesy of Peter Cook, Queen Mary College, London. Elemental analyses were performed by Alfred Bernhard Microanalytische Laboratorium. Cryoscopic molecular weight determinations were done in benzene by using a thermistor incorporated into a bridge circuit.

Reactions with Molecular Oxygen. All reactions between the metal alkoxides and oxygen were carried out in a similar manner. In the drybox, the metal complex was dissolved in a hydrocarbon solvent, and the resultant mixture was placed in a round-bottomed flask containing a Teflon-covered magnetic stirring bar. The flask was fitted with an adapter containing a 2-mm stopcock. The flask was removed from the drybox and attached to a double-manifold vacuum line, consisting of a vacuum and dry molecular oxygen. The solution was frozen at −198 °C (liquid nitrogen) and degassed by thawing in vacuo. The flask was refilled with dry oxygen. The solution was stirred under 1 atm of oxygen (maintained by a mercury bubbler) until the reaction was complete.

Materials. Molecular oxygen was dried prior to use by passing the gas through a U-tube packed with activated molecular sieves. The U-tube was cooled to −78 °C in a dry ice/acetone bath. Isopropyl-d_6 alcohol was prepared by the reduction of acetone-d_6 with LiAlH$_4$, followed by acid hydrolysis, extraction, and distillation. 99% Isotopic purity ^{18}O$_2$ was obtained from Prochem Isotopes.

Preparations. MoO$_2$(O-*t*-Bu)$_2$. Mo$_2$(O-*t*-Bu)$_6$ (104 mg, 0.165 mmol) was dissolved in toluene (15 mL) in a 50-mL round-bottomed flask. The flask was filled with dry oxygen and the solution stirred for 2 h, during which time the color of the solution changed from orange to pale yellow. MoO$_2$(O-*t*-Bu)$_2$ was obtained by stripping the solvent and vacuum distillation of the yellow liquid at 55 °C (10^{-4} torr) (55 mg, 60% yield based on Mo). A cryoscopic molecular weight determination in benzene showed that MoO$_2$(O-*t*-Bu)$_2$ is monomeric in solution, mol wt 267 ± 13 (calculated for MoO$_2$(O-*t*-Bu)$_2$ 274). IR data: 320 m, 370 s, 463 s, 564 s, 587 s, 700 w, 799 s, 930 vs, 968 vs, 1025 s, 1087 m, 1160 vs, 1242 s, 1261 s cm^{-1}.

The average of two gas buret determinations confirmed the stoichiometry of eq 1, O$_2$/Mo$_2$(O-*t*-Bu)$_6$ = 2.0 ± 0.1. When the reaction was done in a sealed NMR tube, a peak appeared at 1.09 ppm in addition to that of MoO$_2$(O-*t*-Bu)$_2$. Addition of *tert*-butyl alcohol enhanced the peak at 1.09 ppm. Vacuum distillation of the volatile components of this reaction into an NMR tube showed that *tert*-butyl alcohol is the only organic product. When the reaction was done with 1,4-cyclohexadiene as the solvent, *tert*-butyl alcohol and benzene were observed in the NMR spectrum in the ratio 2:1. By ^{1}H NMR spectroscopy, formation of MoO$_2$(O-*t*-Bu)$_2$ according to eq 1a appears quantitative.

MoO$_2$(O-*t*-Bu)$_2$(py)$_2$. MoO$_2$(O-*t*-Bu)$_2$ (320 mg, 1.2 mmol) was dissolved in toluene (10 mL) under a nitrogen atmosphere. Pyridine (5.0 mL) was added to the flask with stirring. The solvent and excess pyridine were removed by stripping in vacuo. MoO$_2$(O-*t*-Bu)$_2$(py)$_2$ is a yellow liquid that loses pyridine when heated to 50 °C under vacuum. IR data: 315 s, 351 s, 428 w, 470 s, 610 s, 614 m, 620 w, 691 s, 750 s, 780 s, 920 s, 1030 m, 1068 m, 1160 s, 1210 w, 1230 m, 1570 m, 1594 m cm^{-1}.

MoO$_2$(O-*t*-Bu)$_2$(bpy). MoO$_2$(O-*t*-Bu)$_2$ (220 mg, 0.80 mmol) was dissolved in toluene (25 mL) in a 50-mL round-bottomed flask fitted with a side arm addition tube. 2,2′-Bipyridine (126 mg, 0.80 mmol) was added to the solution via the addition tube with stirring. The solvent was stripped after stirring for 0.5 h, and the white solid was recrystallized from either toluene or methylene chloride (280 mg, 80% yield based on Mo). IR data: 321 s, 382 s, 412 w, 442 m, 467 w, 554 s, 622 w, 644 m, 721 m, 734 s, 750 w, 775 s, 795 w, 888 s, 901 m, 912 s, 935 s, 1021 s, 1055 w, 1098 w, 1150 w, 1172 s, 1221 m, 1253 m, 1310 m, 1575 m, 1595 s cm^{-1}.

MoO$_2$(O-*i*-Pr)$_2$, MoO$_2$(O-*i*-Pr)$_2$(py)$_2$, and MoO$_2$(O-*i*-Pr)$_2$(bpy). Mo$_2$(O-*i*-Pr)$_6$ (1.00 g, 1.83 mmol) was dissolved in toluene (25 mL) in a 100-mL round-bottomed flask under a nitrogen atmosphere. The solution was treated with dry molecular oxygen at 60 °C for 24 h. During this time, the color of the solution changed from yellow to green to brown and finally to pale yellow. MoO$_2$(O-*i*-Pr)$_2$ can be isolated as a white solid by reducing the volume of the solution to ca. 10 mL and adding pentane (25 mL). Cooling the solution causes precipitation of MoO$_2$(O-*i*-Pr)$_2$ as a white solid. Filtration and drying lead to decomposition. The stoichiometry of the overall reaction was determined by a gas buret experiment to be O$_2$/Mo$_2$(O-*i*-Pr)$_6$ = 2.0. When the reaction was done in a sealed vessel in toluene-d_8 and the volatile components were vacuum transferred to an NMR tube, isopropyl alcohol and acetone were identified in the ^{1}H NMR spectrum. When Mo$_2$(O-*i*-Pr)$_6$ was treated with oxygen in 1,4-cyclohexadiene, isopropyl alcohol and benzene were observed in the NMR spectrum in a 2:1 ratio, respectively.

MoO$_2$(O-*i*-Pr)$_2$ is not stable as a solid and decomposes to blue molybdenum oxides even when stored in sealed vials either under N$_2$ or under vacuo. It can, however, be kept in solution for several days before decomposition occurs. Several other methods for preparing MoO$_2$(O-*i*-Pr)$_2$ have been found and are reported below.

MoO$_2$(O-*i*-Pr)$_2$: MoO$_2$(O-*t*-Bu)$_2$ + *i*-PrOH (excess). MoO$_2$(O-*t*-Bu)$_2$ (1.32 g, 4.82 mmol) was dissolved in toluene (25 mL) in a 100-mL round-bottomed flask under a nitrogen atmosphere. Isopropyl alcohol (25 mL) was syringed into the solution while stirring. The solution volume was reduced to ca. 10 mL by stripping in vacuo. Solid MoO$_2$(O-*i*-Pr)$_2$ was isolated by adding pentane (25 mL), cooling, and filtering the white solid.

MoO$_2$(O-*i*-Pr)$_2$: Mo$_6$O$_{10}$(O-*i*-Pr)$_{12}$ + O$_2$. Mo$_6$O$_{10}$(O-*i*-Pr)$_{12}$ (200 mg, 0.138 mmol) was placed in a 25-mL round-bottomed flask under a nitrogen atmosphere. Toluene (10 mL) was added, and the solution was treated with dry molecular oxygen. The solution was stirred at 60 °C until all of the solid had dissolved, approximately 2.5 h. MoO$_2$(O-*i*-Pr)$_2$ was isolated as a white solid by adding pentane (25 mL), cooling, and filtering.

MoO$_2$(O-*i*-Pr)$_2$: Mo$_3$O(O-*i*-Pr)$_{10}$ + O$_2$. Mo$_3$O(O-*i*-Pr)$_{10}$ (ca. 50 mg) was added to an NMR tube and dissolved in toluene-d_8 (0.20 mL). Dry molecular oxygen was added by using a calibrated gas manifold, and the tube was then sealed. The ^{1}H NMR spectrum was taken daily for 3 days, during which time the peaks corresponding to Mo$_3$O(O-*i*-Pr)$_{10}$ declined and those for acetone, isopropyl alcohol, and MoO$_2$(O-*i*-Pr)$_2$ increased in intensity.

MoO$_2$(O-*i*-Pr)$_2$(py)$_2$. As an alternative to isolating the unstable solid MoO$_2$(O-*i*-Pr)$_2$ in the above syntheses, the stable liquid MoO$_2$(O-*i*-Pr)$_2$(py)$_2$ can be isolated by adding pyridine to the flask after preparation. The solvent and excess pyridine are then removed by stripping in vacuo. MoO$_2$(O-*i*-Pr)$_2$(py)$_2$ is a yellow liquid that loses pyridine and begins to decompose when heated to 50 °C in vacuo. IR data: 321 s, 455 s, 610 s, 690 s, 750 s, 794 s, 835 vs, 870 vs, 950 vs, 1031 s, 1064 s, 1100 s, 1155 s, 1212 s, 1322 s, 1480 s, 1575 w, 1601 s cm^{-1}.

MoO$_2$(O-*i*-Pr)$_2$(bpy). MoO$_2$(O-*i*-Pr)$_2$ (0.42 mmol) was prepared by treating MoO$_2$(O-*t*-Bu)$_2$ (0.42 mmol) with *i*-PrOH (excess) in a 50-mL round-bottomed flask fitted with a side arm addition tube under a nitrogen atmosphere. 2,2′-Bipyridine (650 mg, 0.42 mmol) was added to the solution via an addition tube. After the mixture was stirred for 30 min, the solvent was stripped in vacuo and the remaining white solid extracted with toluene (20 mL). The solution volume was reduced, and MoO$_2$(O-*i*-Pr)$_2$(bpy) crystallized by cooling slowly to −10 °C in a freezer. White crystals of MoO$_2$(O-*i*-Pr)$_2$(bpy) were filtered and dried in vacuo (130 mg, ca. 80% based on Mo). MoO$_2$(O-*i*-Pr)$_2$(bpy) can also be recrystallized from methylene chloride. IR data: 316 s, 360 m, 420 m, 432 m, 552 w, 590 s, 623 w, 646 m, 718 w, 732 m, 779 s, 795 w, 835 w, 880 s, 899 s, 960 s, 1020 s, 1054 s, 1109 s, 1158 s, 1258 m, 1310 w, 1569 w, 1592 s cm^{-1}.

MoO$_2$(OCH$_2$-*t*-Bu)$_2$. MoO$_2$(OCH$_2$-*t*-Bu)$_2$ was prepared and isolated from Mo$_2$(OCH$_2$-*t*-Bu)$_6$ in a procedure analogous to the preparation of MoO$_2$(O-*i*-Pr)$_2$ from Mo$_2$(O-*i*-Pr)$_6$ and oxygen. However, MoO$_2$(OCH$_2$-*t*-Bu)$_2$ decomposes very rapidly when isolated as a solid. MoO$_2$(OCH$_2$-*t*-Bu)$_2$ can be stabilized and isolated as an adduct with donor ligands such as pyridine and bpy.

Gas buret experiments confirmed the stoichiometry of the uptake of oxygen: $O_2/Mo_2(OCH_2\text{-}t\text{-}Bu)_6 = 1.8$. When the reaction was done in a sealed vessel in toluene-d_8 and the volatile components were vacuum transferred to an NMR tube, neopentyl alcohol was the only organic product identified. When $Mo_2(OCH_2\text{-}t\text{-}Bu)_6$ was treated with oxygen in 1,4-cyclohexadiene, neopentyl alcohol and benzene were formed in the ratio of 2:1, respectively. Another method for the preparation of $MoO_2(OCH_2\text{-}t\text{-}Bu)_2$ is reported below.

$MoO_2(OCH_2\text{-}t\text{-}Bu)_2$: $Mo_3O(OCH_2\text{-}t\text{-}Bu)_{10}$ + O_2. $Mo_3O(OCH_2\text{-}t\text{-}Bu)_{10}$ (ca. 50 mg) was added to an NMR tube and dissolved in toluene-d_8 (0.25 mL). Dry molecular oxygen was added to the tube by using a calibrated gas manifold, and the tube was sealed. ^1H NMR spectra were recorded periodically over a 4-week period, during which time the peaks that corresponded to $Mo_3O(OCH_2\text{-}t\text{-}Bu)_{10}$ decreased and those for neopentyl alcohol and $MoO_2(OCH_2\text{-}t\text{-}Bu)_2$ increased in intensity. After 5 weeks, the contents of the tube had decomposed to blue molybdenum oxides.

$MoO_2(OCH_2\text{-}t\text{-}Bu)_2(py)_2$. $MoO_2(O\text{-}t\text{-}Bu)_2$ (140 mg, 0.510 mmol) was prepared in toluene (10 mL) in a 50-mL round-bottomed flask from the reaction between $Mo_2(O\text{-}t\text{-}Bu)_6$ (164 mg, 0.260 mmol) and molecular oxygen. A 25-mL portion of a 1.66 M $t\text{-}BuCH_2OH$/toluene solution was added, and the solvent was removed in vacuo until 2 mL of solution remained. Pyridine (10 mL) was syringed into the flask. The solvent and excess neopentyl alcohol were removed by stripping in vacuo. $MoO_2(OCH_2\text{-}t\text{-}Bu)_2(py)_2$ is a yellow liquid that loses pyridine when heated to 50 °C under vacuum. IR data: 307 s, 360 s, 400 m, 459 s, 622 s, 642 m, 731 s, 769 s, 795 w, 890 s, 1018 s, 1040 m, 1052 s, 1098 m, 1145 m, 1175 w, 1220 w, 1249 m, 1285 w, 1313 s, 1570 w, 1590 s, 1601 m cm^{-1}.

$MoO_2(OCH_2\text{-}t\text{-}Bu)_2(bpy)$. $MoO_2(O\text{-}t\text{-}Bu)_2$ (244 mg, 0.892 mmol) was prepared from $Mo_2(O\text{-}t\text{-}Bu)_6$ (281 mg, 0.446 mmol) in toluene (10 mL) in a 50-mL round-bottomed flask fitted with a side arm addition tube. A 30-mL portion of 1.66 M $t\text{-}BuCH_2OH$/toluene solution was added. The solvent was stripped in vacuo until about 2 mL remained. Toluene (15 mL) and 2,2′-bipyridyl (1.39 g, 0.892 mmol) were added. The solvent was stripped and the remaining white solid recrystallized from toluene (300 mg, ca. 75% yield based on Mo). IR data: 305 s, 367 s, 401 m, 412 w, 461 s, 620 s, 644 m, 732 s, 770 s, 795 w, 892 s, 918 s, 1018 s, 1044 m, 1058 s, 1088 w, 1148 m, 1170 w, 1220 w, 1252 m, 1287 w, 1313 s, 1570 w, 1592 s, 1600 m cm^{-1}.

$MoO(O\text{-}t\text{-}Bu)_4$. $Mo(O\text{-}t\text{-}Bu)_4$ (1.00 g, 2.58 mmol) was dissolved in toluene (10 mL) in a 50-mL round-bottomed flask under a nitrogen atmosphere. Oxygen was added to the flask and the solution stirred at room temperature (1 atm) for 3 h. During this time, the color of the solution changed from green to yellow. The solvent was stripped to yield a thick yellow oil. $MoO(O\text{-}t\text{-}Bu)_4$ was obtained as a yellow liquid by vacuum distillation at 85 °C (10^{-4} torr) (404 mg, ca. 40% yield based on Mo). IR data: 329 m, 365 s, 463 s, 562 s, 595 s, 691 w, 709 w, 741 w, 775 m, 790 m, 967 vs, 1020m, 1090 w, 1160 s, 1235 s cm^{-1}.

$MoO(O\text{-}i\text{-}Pr)_4$. $Mo_2(O\text{-}i\text{-}Pr)_8$ (1.80 g, 2.71 mmol) was dissolved in toluene (25 mL) in a 50-mL round-bottomed flask under a nitrogen atmosphere. Oxygen was added to the flask and the solution stirred for 1 h (1 atm of O_2). During this time, the color changed from blue to green to yellow. The solvent was stripped to yield a thick yellow oil. $MoO(O\text{-}i\text{-}Pr)_4$ was obtained as a yellow liquid by vacuum distillation at 60 °C (10^{-4} torr) (720 mg, ca. 40% yield based on Mo). IR data: 325 m, 391 w, 465 m, 495 w, 601 s, 815 s, 840 s, 951 s, 1010 w, 1100 s, 1162 s, 1254 s, 1318 s, 1360 s, 1375 s, 1448 m, 1460 m cm^{-1}.

$MoO(OCH_2\text{-}t\text{-}Bu)_4$. $[Mo(OCH_2\text{-}t\text{-}Bu)_4]_x$ (348 mg, 0.780 mmol) was dissolved in toluene (50 mL) in a 100-mL round-bottomed flask under a nitrogen atmosphere. Dry molecular oxygen was added to the flask. While the mixture was stirred for 2 h under O_2 (1 atm) at room temperature, the color changed from blue to green to yellow. The solvent was stripped to give a yellow solid. $MoO(OCH_2\text{-}t\text{-}Bu)_4$ was obtained by sublimation at 75–85 °C (10^{-4} torr) using a dry ice/acetone cooled probe (210 mg, 60% yield based on Mo). IR data: 300 w, 342 m, 399 m, 421 s, 509 s, 582 s, 619 s, 651 s, 683 s, 719 w, 749 m, 796 w, 915 s, 930 s, 990 s, 1018 s, 1035 s, 1212 m, 1260 m, 1290 w cm^{-1}.

$Mo_3O(O\text{-}i\text{-}Pr)_{10}$. $MoO(O\text{-}i\text{-}Pr)_4$ (640 mg, 1.84 mmol) was dissolved in toluene (25 mL) in a 50-mL round-bottomed flask fitted with a side arm addition tube under a nitrogen atmosphere. $Mo_2(O\text{-}i\text{-}Pr)_6$ (1.0 g, 1.84 mmol) was added via the side arm addition tube with stirring. The solution immediately turned from yellow to red and then to green. The solution was stirred for 1 h at room temperature and then the solvent was stripped. The green solid was recrystallized from methylene chloride. Green crystals of $Mo_3O(O\text{-}i\text{-}Pr)_{10}$ were filtered from the solution and dried in vacuo (1.08 g, 65% yield). IR data: 320 m, 460 w, 605 s, 818 m, 846 s, 930 s, 963 s, 1105 s, 1160 m, 1259 w, 1311 m, 1322 m cm^{-1}.

$Mo_3O(OCH_2\text{-}t\text{-}Bu)_{10}$. $MoO(OCH_2\text{-}t\text{-}Bu)_4$ (96 mg, 0.209 mmol) was dissolved in toluene (30 mL) in a 50-mL round-bottomed flask fitted with a side arm addition tube under a nitrogen atmosphere. $Mo_2(OCH_2\text{-}t\text{-}Bu)_6$ (149 mg, 0.209 mmol) was added via the side arm addition tube with stirring. The color of the solution immediately changed from yellow to green. The solution was stirred for 1.5 h at room temperature. The solvent was stripped in vacuo. The remaining green solids were crystallized from hexane. Green crystals of $Mo_3O(OCH_2\text{-}t\text{-}Bu)_{10}$ were filtered from the solution and dried in vacuo (170 mg, ca. 70% yield). IR data: 354 w, 400 w, 465 w, 632 s, 655 m, 670 m, 715 w, 750 m, 795 m, 864 w, 928 w, 1012 s, 1039 s, 1210 s, 1255 s, 1290 m cm^{-1}.

$Mo_6O_{10}(O\text{-}i\text{-}Pr)_{12}$: $Mo_2(O\text{-}i\text{-}Pr)_6$ + O_2. $Mo_2(O\text{-}i\text{-}Pr)_6$ (227 mg, 0.416 mmol) was dissolved in toluene (25 mL) in a 50-mL round-bottomed flask under a nitrogen atmosphere. The flask was filled with dry molecular oxygen and the solution stirred for 2 h at room temperature. During this time, the color of the solution changed from yellow to green. The solution was frozen at −198 °C (liquid nitrogen) and the oxygen removed by thawing in vacuo. The flask was refilled with nitrogen and the solution stirred for 1 week at room temperature. Pentane (20 mL) was added to the flask, and it was cooled to −10 °C in a freezer. Yellow crystals of $Mo_6O_{10}(O\text{-}i\text{-}Pr)_{12}$ precipitated overnight and were filtered and dried in vacuo (65 mg). IR data: 395 m, 453 w, 473 m, 499 m, 555 w, 608 s, 642 m, 621 w, 640 w, 655 w, 822 s, 842 m, 850 m, 932 vs, 953 s, 986 s, 1099 s, 1118 s, 1170 w, 1260 w, 1319 m cm^{-1}.

$Mo_6O_{10}(O\text{-}i\text{-}Pr)_{12}$: $Mo_2(O\text{-}i\text{-}Pr)_8$ + $MoO_2(O\text{-}i\text{-}Pr)_2$. $MoO_2(O\text{-}i\text{-}Pr)_2$ (250 mg, 1.02 mmol) was prepared in toluene (30 mL) by alcoholysis of $MoO_2(O\text{-}t\text{-}Bu)_2$ (279 mg, 1.02 mmol) in a 50-mL round-bottomed flask equipped with a side arm addition tube. $Mo_2(O\text{-}i\text{-}Pr)_8$ (113 mg, 0.170 mmol) was added to the yellow solution. Upon mixing, the solution turned brown and yellow crystals of $Mo_6O_{10}(O\text{-}i\text{-}Pr)_{12}$ began to precipitate. The flask was cooled to −10 °C in a freezer. Yellow crystals of $Mo_6O_{10}(O\text{-}i\text{-}Pr)_{12}$ were filtered and dried in vacuo (ca. 150 mg).

$Mo_6O_{10}(O\text{-}i\text{-}Pr)_{12}$: $Mo_3O(O\text{-}i\text{-}Pr)_{10}$ + $MoO_2(O\text{-}i\text{-}Pr)_2$. $MoO_2(O\text{-}i\text{-}Pr)_2$ (177 mg, 0.720 mmol) was prepared in toluene (20 mL) by alcoholysis of $MoO_2(O\text{-}t\text{-}Bu)_2$ (198 mg, 0.720 mmol) in a 50-mL round-bottomed flask equipped with a side arm addition tube. $Mo_3O(O\text{-}i\text{-}Pr)_{10}$ (80 mg, 0.90 mmol) was added to the solution via the addition tube. The mixture was stirred for 1 week at 45 °C (1 atm of N_2), during which time the color changed from green to brown and yellow crystals began to form. The flask was placed in a freezer at −10 °C. Yellow crystals of $Mo_6O_{10}(O\text{-}i\text{-}Pr)_{12}$ formed overnight and were filtered and dried in vacuo (ca. 200 mg).

$Mo_4O_8(O\text{-}i\text{-}Pr)_4(py)_4$: $Mo_2(O\text{-}i\text{-}Pr)_6$ + O_2 + py. $Mo_2(O\text{-}i\text{-}Pr)_6$ (160 mg, 0.29 mmol) was dissolved in pyridine (20 mL) in a 50-mL round-bottomed flask under a nitrogen atmosphere. The flask was filled with molecular oxygen, and the solution was allowed to stand for 12 h at room temperature (1 atm of O_2). During this time, the solution changed from green to yellow and a small quantity of a red crystalline solid formed. The red solid was filtered and dried in vacuo (ca. 50 mg). IR data: 320 m, 340 w, 394 w, 418 w, 431 m, 469 s, 501 w, 566 m, 597 s, 634 m, 653 s, 682 s, 722 s, 750 s, 810 m, 830 m, 914 s, 949 vs, 968 s, 1011 m, 1021 w, 1039 m, 1065 m, 1115 vs, 1154 m, 1212 s, 1312 m, 1572 m, 1601 s cm^{-1}.

$Mo_4O_8(O\text{-}i\text{-}Pr)_4(py)_4$: $Mo_6O_{10}(O\text{-}i\text{-}Pr)_{12}$ + py (excess). $Mo_6O_{10}(O\text{-}i\text{-}Pr)_{12}$ (50 mg, 0.034 mmol) was placed into a 10-mL round-bottomed flask under a nitrogen atmosphere. Pyridine (1.0 mL) was added to the flask. The yellow solid slowly dissolved to form a red solution. The flask was cooled slowly to −10 °C. Red crystals of $Mo_4O_8(O\text{-}i\text{-}Pr)_4(py)_4$ formed overnight and were filtered and dried in vacuo (ca. 30 mg).

X-ray Structure Determinations. The diffractometers used in this study are upgraded versions of the instrument described in a previous work.[49] The new instrument eliminates the discrete logic circuitry

---

(49) Huffman, J. C.; Lewis, L. N.; Caulton, K. G. *Inorg. Chem.* **1980**, *19*, 2755.

Table XVII. Summary of Crystallographic Data[a]

	I	II	III	IV
fw	448.37	1260.17	894.70	1444.69
space group	$P\bar{1}$	*Pbcn*	$P\bar{1}$	$P\bar{1}$
a, Å	13.907 (6)	35.557 (19)	21.274 (6)	13.082 (3)
b, Å	8.413 (3)	18.969 (9)	21.808 (5)	11.478 (2)
c, Å	19.999 (8)	19.342 (9)	10.207 (2)	9.760 (2)
α, deg	111.02 (1)		98.69 (1)	106.40 (1)
β, deg	71.37 (2)		92.92 (1)	91.85 (1)
γ, deg	88.98 (1)		118.03 (1)	99.81 (1)
Z	4	8	4	1
V, Å^3	2046.39	13045.59	4091.77	1380.34
d_{calcd}, g/cm^3	1.455	1.283	1.452	1.738
cryst dimens, mm	0.13 × 0.14 × 0.12	0.12 × 0.14 × 0.16	0.08 × 0.16 × 0.25	0.22 × 0.21 × 0.26
cryst color	brownish	green	green	orange
radiation	Mo Kα (λ = 0.710 69 Å) graphite monochromator			
linear abs coeff, cm^{-1}	6.49	6.83	9.30	13.57
temp, °C	−161	−161	−162	−162
instrument	Picker 4-circle diffractometer locally modified and interfaced			
detector aperture	3.0 mm wide × 4.0 mm high; 22.5 cm from crystal			
sample to source dist	23.5 cm			
takeoff angle, deg	2.0	2.0	2.0	2.0
scan speed, deg/min	3.5	2.5	3.0	5.0
scan width,[c] deg	1.7	1.0	2.0	2.0
bkgd count,[b] s	3	3	4	3
2θ range, deg	6–45	6–40	6–40	6–50
data collcd	5694	10 379	11 676	5643
no. of unique data	5353	6102	10 717	4891
no. of unique data $F_o > 3\sigma(F_o)$	4021	2830	7711	4388
no. of variables	469	293	793	457
R(*F*)	0.067	0.075	0.070	0.027
$R_w(F)$	0.068	0.076	0.066	0.036
goodness of fit	1.494	1.558	1.358	1.171
largest Δ/σ	0.05	0.04	0.05	0.03

[a] I = $MoO_2(O\text{-}i\text{-}Pr)_2(bpy)\cdot{}^1/_2(toluene)$; II = $Mo_3O(OCH_2\text{-}t\text{-}Bu)_{10}\cdot{}^1/_3CH_2Cl_2$; III = $Mo_3O(O\text{-}i\text{-}Pr)_{10}$; IV = $Mo_6O_{10}(O\text{-}i\text{-}Pr)_{12}$. [b] At the end of each scan. [c] All plus dispersion correction of 0.692 tan θ.

previously used for the timer/scaler, shutter control, and motor drive functions and instead uses a custom-built Z80 microcomputer with appropriate programmable interfaces. A serial interface allows bidirectional communication between the Z80 and the Texas Instruments TI980B minicomputer which is used for computing angular settings and overall control of the goniostat. Each TI980B is equipped with dual 8-in. floppy diskette drives for program and data storage, as well as several serial interfaces that are used for communication to other computers and peripheral devices in the laboratory network.

The Z80 software includes an automatic search routine that can be programmed to systematically examine a specified region of reciprocal space on the goniostat to locate diffraction maxima. Other Z80 software allows continuous plotting of the peak profile on a CRT terminal during data collection. Data collection can be performed at virtually any scan rate using normal θ–2θ scans, ω scans, or fixed θ–2θ modes. Complete details of the diffractometer interface and laboratory computer network will be published elsewhere.[50] The low-temperature apparatus and data reduction techniques do not differ significantly from the earlier description.[49,51]

$MoO_2(O\text{-}i\text{-}Pr)_2(bpy)\cdot{}^1/_2C_7H_8$. A suitable crystal was transferred to the goniostat and cooled to −161 C. A systematic search of reciprocal space revealed no systematic absences or symmetry-related reflections, indicating a triclinic space group. Crystal and diffractometer data are summarized in Table XVII.

The structure was solved by a combination of direct methods and Fourier techniques. Two independent molecules were located in the asymmetric cell as well as disordered toluene solvent molecules. During the course of the refinement, one of the $MoO_2(O\text{-}i\text{-}Pr)_2(bpy)$ molecules was discovered to have a disordered O-*i*-Pr group, with three possible configurations for the methyl groups. Because of the disorder problems, no attempt was made to locate or refine hydrogen atoms. A final difference Fourier contained numerous peaks of intensity 0.3–0.9 e/Å^3, many of which were in likely positions for hydrogens. Anisotropic thermal parameters, a complete listing of distances and angles, and observed and calculated structure amplitudes are available as supplementary material.

$Mo_3O(OCH_2\text{-}t\text{-}Bu)_{10}\cdot xCH_2Cl_2$. A suitable crystal was mounted as above, and a systematic search revealed a set of maxima with orthorhombic symmetry and extinctions that could be indexed as *Pbcn*. Crystal and diffractometer data are given in Table XVII. The structure was solved by direct methods and Fourier techniques. A rather large percentage of the data (45%) were unobserved by using the criteria $I_o \geq 2.33\sigma(I_o)$. This was apparently due to a loss of a solvent molecule (CH_2Cl_2) and a disorder in one of the OCH_2-*t*-Bu groups. While the disorder in the latter was clearly discernible in regular and difference Fourier maps, attempts to properly refine a disordered model led to unrealistic interatomic distances and angles. The partial occupancy solvent molecule was located in a difference Fourier after examination of the molecular packing revealed a void of nearly 9 Å diameter in the structure. While the carbon atom of the solvent was not locatable, the two chlorine atoms refined to an average occupancy of 0.33. No attempt was made to locate hydrogen atoms, and a final difference Fourier gave a nearly random distribution of peaks of intensity up to 0.7 e/Å^3. Anisotropic thermal parameters, complete listings of bonded distances and angles, and observed and calculated structure amplitudes are available as supplementary material.

$Mo_3O(O\text{-}i\text{-}Pr)_{10}$. A suitable crystal was cooled to −162 °C, and a reciprocal lattice search revealed no systematic absences or symmetry, indicating a triclinic lattice. Crystal and diffractometer data are given in Table XVII. Two independent molecules were located by a combination of direct methods and Fourier techniques. Due to the number of atoms in the cell, the structure was refined in blocks during the full-matrix refinement. No attempt was made to locate or refine hydrogen atoms, although many were apparent in a final difference Fourier synthesis. A least-squares fit[52] of the molecular framework

---

(50) Huffman, J. C. Ph.D. Thesis, Indiana University, Bloomington, IN, 1974.

(51) Huffman, J. C.; Streib, W. E.; Sporleder, C. R., in preparation.

(52) Nyburg, S. C. *J. Appl. Crystallogr.* **1979**, 117.

(53) Ardon, M.; Cotton, F. A.; Dori, Z.; Fang, A.; Kapon, M.; Reisner, G. M.; Shaia, M. *J. Am. Chem. Soc.* **1982**, *104*, 5394.

(54) Cotton, F. A.; Morehouse, S. M. *Inorg. Chem.* **1965**, *4*, 1377.

(55) Knox, J. R.; Prout, C. K. *Acta Crystallogr. Sect. B* **1969**, *25B*, 1857.

of the two independent molecules and the framework of the $Mo_3O(OCH_2\text{-}t\text{-}Bu)_{10}$ molecule indicates the inner coordination geometry of the three are essentially identical. Anisotropic thermal parameters, complete listings of distances and angles, the molecular fit least squares, and observed and calculated structure amplitudes are available as supplementary material.

$Mo_6O_{10}(O\text{-}i\text{-}Pr)_{12}$. A triclinic lattice was located in the diffraction maxima collected at −161 °C. The structure was readily solved by a combination of Patterson and Fourier techniques. Crystal and diffractometer data are given in Table XVII. Since there is only one molecule in the centrosymmetric space group, the molecule possesses crystallographic as well as molecular C_i symmetry. All hydrogen atoms were located in a difference Fourier phased on the non-hydrogen parameters and were allowed to vary isotropically for the final refinement. A final difference Fourier was featureless, with the largest peak being 0.5 e/Å^3. Anisotropic thermal parameters, hydrogen coordinates, complete distances and angles, and a listing of observed and calculated structure amplitudes are available as supplementary material.

Acknowledgment. We thank the Office of Naval Research for support of this work. M.H.C. is a recipient of a Henry and Camille Dreyfus Teacher-Scholar grant, 1979–1984, and C.C.K. is the Indiana University SOHIO Fellow, 1979–1982.

Registry No. I, 89015-24-7; II, 88947-09-5; III, 79256-75-0; IV, 83419-17-4; $MoO_2(O\text{-}t\text{-}Bu)_2$, 78134-32-4; $MoO_2(O\text{-}t\text{-}Bu)_2(bpy)$, 88916-52-3; $MoO_2(O\text{-}i\text{-}Pr)_2(bpy)$, 88979-78-6; $MoO_2(OCH_2\text{-}t\text{-}Bu)_2(bpy)$, 88916-55-6; $MoO(O\text{-}t\text{-}Bu)_4$, 88916-58-9; $MoO(O\text{-}i\text{-}Pr)_4$, 79210-24-5; $MoO(OCH_2\text{-}t\text{-}Bu)_4$, 79218-12-5; $Mo_3O(OCH_2\text{-}t\text{-}Bu)_{10}$, 88947-08-4; $Mo_4O_8(O\text{-}i\text{-}Pr)_4(py)_4$, 88916-56-7; $MoO_2(O\text{-}t\text{-}Bu)_2(py)_2$, 88916-51-2; $MoO_2(O\text{-}i\text{-}Pr)_2(py)_2$, 88916-53-4; $MoO_2(OCH_2\text{-}t\text{-}Bu)_2(py)_2$, 88916-54-5; $MoO_2(O\text{-}i\text{-}Pr)_2$, 82123-87-3; $MoO_2(OCH_2\text{-}t\text{-}Bu)_2$, 88916-57-8; $Mo_2(O\text{-}t\text{-}Bu)_6$, 60764-63-8; $Mo_2(O\text{-}i\text{-}Pr)_6$, 62521-20-4; $Mo_2(OCH_2\text{-}t\text{-}Bu)_6$, 62521-24-8; $Mo(O\text{-}t\text{-}Bu)_4$, 60624-53-5; $Mo_2(O\text{-}i\text{-}Pr)_8$, 66526-46-3; $[Mo(OCH_2\text{-}t\text{-}Bu)_4]_x$, 66917-89-3; O_2, 7782-44-7.

Supplementary Material Available: Listings of fractional coordinates, isotropic and anisotropic thermal parameters, and complete bond distances and angles, stereoviews, and listings of observed and calculated structure amplitudes for the single-crystal structural studies for all the compounds and a listing of hydrogen coordinates for $Mo_6O_{10}(O\text{-}i\text{-}Pr)_{12}$ (215 pages). Ordering information is given on any current masthead page. Complete crystallographic data are also available, in microfiche form only, from the Indiana University Chemistry Library, Bloomington, IN 47405. Request MSC Report No. 81047 for $MoO_2(O\text{-}i\text{-}Pr)_2(bpy)$, No. 81006 for $Mo_3O(OCH_2\text{-}t\text{-}Bu)_{10}$, No. 81029 for $Mo_3O(O\text{-}i\text{-}Pr)_{10}$, and No. 81025 for $Mo_6O_{10}(O\text{-}i\text{-}Pr)_{12}$ when ordering.

---

(56) Drew, M. G. B.; Kay, A. *J. Chem. Soc. A* **1971**, 1846.

Contribution from the Department of Chemistry and Molecular Structure Center,
Indiana University, Bloomington, Indiana 47405

Reactions of Metal–Metal Multiple Bonds. 11.[1] A Comparison of the Reactivity of $M_2(OR)_6$ (M≡M) and $M_2(OR)_4(R'COCHCOR')_2$ (M≡M) Compounds (M = Mo, W) with the π-Acid Ligands CO, RC≡CR, and RNC

MALCOLM H. CHISHOLM,* JAMES F. CORNING, KIRSTEN FOLTING, JOHN C. HUFFMAN,
ANDREW L. RATERMANN, IAN P. ROTHWELL,[2] and WILLIAM E. STREIB

Received June 24, 1983

$M_2(OR)_6$ compounds (M = Mo, W; R = *t*-Bu, *i*-Pr, CH_2-*t*-Bu) react in hydrocarbon solvents with isocyanide ligands to give, upon workup with methanol and KPF_6, $M(CN\text{–alkyl})_7^{2+}$ salts or $M(CNPh)_6$ compounds in a similar manner, noted by Walton and co-workers for reactions involving M–M quadruply bonded compounds. By contrast, $Mo_2(OR)_4(R'COCHCOR')_2$ compounds (R′ = Me, *t*-Bu) react in hydrocarbon solvents to give edge-shared (μ-OR) octahedral complexes and provide the first examples of the conversion of $L_4M{\equiv}ML_4$ compounds to $L_4M(\mu\text{-}L)_2ML_4$ compounds. These are also the first reactions wherein a multiple bond between molybdenum atoms is not cleaved by isocyanide ligands. The compound $Mo_2(OCH_2\text{-}t\text{-}Bu)_4(MeCOCHCOMe)_2(t\text{-}BuNC)_2$ has been fully characterized by an X-ray study. Cell dimensions at −163 °C are a = 13.817 (5) Å, b = 12.518 (4) Å, c = 14.045 (5) Å, and β = 92.61 (2)° with Z = 2 in the space group $P2_1/n$. The conversion of an unbridged triple bond $\sigma^2\pi^4$ to an edge-bridged d^3–d^3 dimer of formal M–M configuration $\sigma^2\pi^2\delta^2$ is accompanied by an increase in Mo–Mo distance, 2.237 (1)–2.508 (2) Å. Related ditungsten alkoxide β-diketonates (M≡M) fail to react with *t*-BuNC under comparable conditions. Both molybdenum and tungsten alkoxide β-diketonates fail to react with CO and alkynes under conditions wherein $M_2(OR)_6$ and $M_2(OR)_6(L)_2$ compounds yield $M_2(\mu\text{-}X)$ derivatives (X = CO, alkynes) or products of cleavage of the M–M bond. $Mo_2(OCH_2\text{-}t\text{-}Bu)_4(MeCOCHCOMe)_2$ reacts with 2,2′-bipyridine to give $Mo_2(OCH_2\text{-}t\text{-}Bu)_4(MeCOCHCOMe)_2(bpy)$, which, on the basis of ^1H NMR spectroscopy, is proposed to be an edge-shared (μ-OR) bioctahedral compound. The marked differences in reactivity of $M_2(OR)_6$ and the mixed alkoxide β-diketonate complexes are discussed in terms of kinetic and/or thermodynamic factors.

Introduction

In a previous paper, we described[3] the preparation and characterization of mixed alkoxide–β-diketonate complexes, $M_2(OR)_4(R'COCHCOR'')_2$, which contained two four-ligated metal atoms (M = Mo, W) united by an unbridged M≡M bond. These are schematically represented by I. Both the formal negative charge and the chelate effect serve to keep the metal atoms four-ligated in hydrocarbon solvents, and only at +110 °C for M = Mo is there any evidence for rapid reversible bidentate ⇌ monodentate behavior of the β-di-

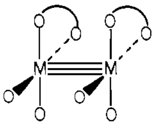
I

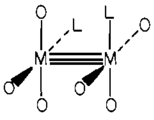
II

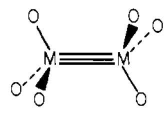
III

O = OR, $\widehat{O\ O}$ = β-diketonate

---

[1] Part 10: Chisholm, M. H.; Folting, K.; Huffman, J. C.; Kirkpatrick, C. C. *Inorg. Chem.*, preceding paper in this issue.

[2] Present address: Purdue University, West Lafayette, IN 47907.

[3] Chisholm, M. H.; Huffman, J. C.; Ratermann, A. L. *Inorg. Chem.* **1983**, *22*, 4100.